

Hawaii National Marine Renewable Energy Center (HINMREC)

U.S. Department of Energy Award Number:
DE-FG36-08GO18180

Task 5: Wave Energy Conversion Device Performance

WEC Ocean Testing: Performance Model Verification, Progress Report 1

Prepared by:
DNV GL Energy

Prepared for:
Hawaii Natural Energy Institute, University of Hawaii

March 2016



HAWAII NATIONAL MARINE RENEWABLE ENERGY CENTER - WEC
OCEAN TESTING

WEC Performance Model Verification - Progress Report #1

Hawaii Natural Energy Institute (HNEI)

Report No.: 702053-USSD-T-03, Rev. B

Date: 4 March 2016



IMPORTANT NOTICE AND DISCLAIMER

1. This document is intended for the sole use of the Client as detailed on the front page of this document to whom the document is addressed and who has entered into a written agreement with the DNV GL entity issuing this document ("DNV GL"). To the extent permitted by law, neither DNV GL nor any group company (the "Group") assumes any responsibility whether in contract, tort including without limitation negligence, or otherwise howsoever, to third parties (being persons other than the Client), and no company in the Group other than DNV GL shall be liable for any loss or damage whatsoever suffered by virtue of any act, omission or default (whether arising by negligence or otherwise) by DNV GL, the Group or any of its or their servants, subcontractors or agents. This document must be read in its entirety and is subject to any assumptions and qualifications expressed therein as well as in any other relevant communications in connection with it. This document may contain detailed technical data which is intended for use only by persons possessing requisite expertise in its subject matter.
2. This document is protected by copyright and may only be reproduced and circulated in accordance with the Document Classification and associated conditions stipulated or referred to in this document and/or in DNV GL's written agreement with the Client. No part of this document may be disclosed in any public offering memorandum, prospectus or stock exchange listing, circular or announcement without the express and prior written consent of DNV GL. A Document Classification permitting the Client to redistribute this document shall not thereby imply that DNV GL has any liability to any recipient other than the Client.
3. This document has been produced from information relating to dates and periods referred to in this document. This document does not imply that any information is not subject to change. Except and to the extent that checking or verification of information or data is expressly agreed within the written scope of its services, DNV GL shall not be responsible in any way in connection with erroneous information or data provided to it by the Client or any third party, or for the effects of any such erroneous information or data whether or not contained or referred to in this document.
4. Any wind or energy forecasts estimates or predictions are subject to factors not all of which are within the scope of the probability and uncertainties contained or referred to in this document and nothing in this document guarantees any particular wind speed or energy output.

KEY TO DOCUMENT CLASSIFICATION

Strictly Confidential	:	For disclosure only to named individuals within the Client's organisation.
Private and Confidential	:	For disclosure only to individuals directly concerned with the subject matter of the document within the Client's organisation.
Commercial in Confidence	:	Not to be disclosed outside the Client's organisation.
DNV GL only	:	Not to be disclosed to non-DNV GL staff
Client's Discretion	:	Distribution for information only at the discretion of the Client (subject to the above Important Notice and Disclaimer and the terms of DNV GL's written agreement with the Client).
Published	:	Available for information only to the general public (subject to the above Important Notice and Disclaimer).

Project name:	Hawaii National Marine Renewable Energy Center - WEC Ocean Testing	DNV GL Energy Renewables Advisory Americas 9665 Chesapeake Drive Suite 435 San Diego CA 92123 USA Tel: +1 858 836 3370 Registered in America No. 94-3402236
Report title:	WEC Performance Model Verification - Progress Report #1	
Customer:	Hawaii Natural Energy Institute (HNEI)	
Contact person:	Luis Vega	
Date of issue:	04 March 2016	
Project No.:	702053	
Report No.:	702053-USSD-T-03, Rev. B	

Task and objective: Provide wave energy converter (WEC) performance and loading simulation data for verification of HNEI's WEC performance model.

Prepared by:

Verified by:

Approved by:

John Roadnight
Engineer - Wave & Tidal Energy

Ben Child
Engineer - Wave & Tidal Energy

Ricard Buils Urbano
Head of Section - Wave & Tidal Energy

- Strictly Confidential
- Private and Confidential
- Commercial in Confidence
- DNV GL only
- Client's Discretion
- Published

Keywords:
Performance, Loading, Size optimization

Reference to part of this report which may lead to misinterpretation is not permissible.

Rev. No.	Date	Reason for Issue	Prepared by	Verified by	Approved by
A	29/01/2016	First issue	J Roadnight	B Child	E Mackay
B	04/03/2016	Revised issue incorporating feedback from HNEI	B Child	R Buils Urbano	R Buils Urbano



Table of contents

1	EXECUTIVE SUMMARY	2
2	INTRODUCTION	4
3	WEC DEFINITION	7
3.1	Overview of scaling methodology	7
3.2	Definition of the generic single body point absorber	9
3.3	PTO damping	10
3.4	Scaling range	11
4	WAVEDYN MODEL	13
4.1	Theory	13
4.2	Structural Model	14
4.3	Hydrodynamic Model	17
4.4	Sea states	19
5	POST PROCESSING FOR WEC PERFORMANCE	23
6	WEC PERFORMANCE RESULTS	25
7	CALCULATION OF STRUCTURAL MASS	29
7.1	Design loads	29
7.2	Plate thickness requirement	33
7.3	Structural mass	34
8	COST PER MW OF RATED POWER OUTPUT	40
9	CONCLUSIONS	44
10	REFERENCES	46

1 EXECUTIVE SUMMARY

The objective of this technical note is to document progress towards providing wave energy converter (WEC) performance and loading simulation data for verification of the University of Hawaii, Hawaii Natural Energy Institute (UH HNEI)'s WEC performance model.

A time-domain numerical model has been created of a *generic rounded cylinder single-body point absorber* in DNV GL's WaveDyn WEC design tool and run for a broad range of unidirectional sea states. WaveDyn has been subjected to a range of validation exercises and was developed specifically for WECs. The results of this model can therefore be used by HNEI to verify their own numerical models and gain understanding on the behaviors of this simple type of WEC device, before progressing to verification and validation on more complex types of device.

The model represents a single scale of device, but Froude scaling rules have been used to generate equivalent results for a range of sizes (scales) of the device, representing a buoy diameter from 2.5m up to 40m. This approach is highly efficient in regard to simulation time and allows results for a large number of device sizes to be compared.

A summary of the power performance results for the modelled WEC is given in section 6 of this progress report. The full set of results will be provided in subsequent deliverables for this phase of work. The annual mean power absorbed for the range of buoy sizes, from 2.5m to 40m diameter, is presented for two site locations, Wave Energy Test Site (WETS) in Hawaii and the European Marine Energy Centre (EMEC) of the Orkney Islands in the UK. The mean annual power is shown to increase with device scale, which is explained in two ways. The first is that wave resource (energy flux per unit width) for a given wave amplitude increases with wavelength and the larger diameter devices resonate at larger periods of oscillation. Also, the resonant period for the larger devices (around 20m) are shown to coincide with the most frequently occurring waves for the two sites.

HNEI has expressed interest in understanding whether different optimum sizes of device can be chosen for different site locations (e.g. would a relatively small WEC be more appropriate for the WETS site, where shorter energy periods are more frequent, as opposed to other more exposed locations).

The relationship between annual mean absorbed power and device scale has been used as the basis for a high-level study into optimum device scale, based on minimum *Cost per MW rated power*. This allows for the performance of different scales of device to be compared *both* in regard to relative power performance and cost for survivability.

As discussed in section 8, a full cost analysis would normally involve detailed analysis of individual capital, operational and balance of plant costs. For this high-level study, the focus is on understanding the relative influence of costs that scale with the device and those that are relatively constant with scale. Therefore, the approach has been to assume costs can be divided into these two main components: scalable and non-scalable (i.e. 'fixed') costs. An example exercise has been carried out for estimating the mass and cost of the main buoy structure for different scales of device. This has then been used as the basis for estimating the overall scalable costs for the device. Although the current example is necessarily based on simplifying assumptions, it is suggested that the process can be used as the basis for future work, where HNEI might use similar methods to estimate the scalable costs of other WEC components.

For the current WEC, it is found that calculated mean annual power absorbed initially increases at a faster rate than cost with scale for devices below approximately 5 to 10m diameter. However for larger sizes of device, the scalable cost of the buoy structure is found to increase at a faster rate than the mean power. This means that an optimum buoy size may be found that minimizes Cost per MW rated



power. Although, as previously stated, this represents a first-pass methodology it can be seen that a similar approach may prove useful in sizing devices for specific wave climates.

2 INTRODUCTION

This technical note is issued to the Research Corporation of the University of Hawaii (RCUH or the "Client") pursuant to a written Agreement for Services effective 14 March 2013 and RCUH Purchase Order #Z10027978 [1] as well as the subsequent amendment to the agreement [2]. The Client has requested that Garrad Hassan America, Inc. (DNV GL) perform services relating to the establishment of a wave energy test center for the University of Hawaii, Hawaii Natural Energy Institute (UH HNEI). UH HNEI's Hawaii National Marine Renewable Energy Center (HINMREC), under funding from the U.S. Department of Energy (DOE) is working in collaboration with the U.S. Navy to develop the Wave Energy Test Site (WETS or the "Project") located at U.S. Marine Corps Base Hawaii – Kaneohe (MCBH-K) in Oahu, Hawaii.

The project consists of three main components [1]:

1. Documentation of test protocols and support to the testing program
2. Provision of data for verification of WEC performance models
3. Provision of data for verification of WEC array models

The present technical note forms part of the *second* project component.

As per the service agreement [1], the scope of the second component of the project is to use DNV GL's in-house WEC performance and loading analysis tool WaveDyn to assist with the verification of HNEI's WEC performance model. WaveDyn has been subjected to a range of validation exercises and was developed specifically for WECs. The tool allows for flexible, multi-body modelling of a wide range of WEC concepts in time domain simulations and couples loading from critical areas including hydrodynamics, power take off, and moorings.

Initially it was intended that HNEI would supply outputs from their own performance models for a series of real WEC devices being tested at the WETS site and DNV GL would generate independent models and simulations for comparison. However, due to the lack of availability of data relating to the devices being tested at WETS and following discussion with HNEI, it has been agreed [5] that DNV GL will instead simulate a range of *generic* WEC models in conditions representative of the WETS site in order to provide a database of results for later use by HNEI.

An advantage of basing this work on a range of generic WEC devices is that the definition of each model can be chosen to clearly demonstrate a variety of physical phenomena that are important to capture by any numerical model. Also, the chosen models can be based on other previous physical or numerical validation work, which is beneficial for cross-referencing of results.

Furthermore, it has been agreed between DNV GL and HNEI [5] that the technical support to the testing programme detailed in [1] under deliverables 5.1 and 5.2 would most usefully take the form of providing further verification data for HNEI's numerical models. This will allow increased confidence in the numerical predictions generated by HNEI and thus enhance understanding of the data relating to the WECs that are installed at WETS.

Therefore, the present phase of work (provision of data for verification of WEC performance models) will be associated with five deliverables:

1. WEC performance model verification progress report #1
2. Testing support progress report #1

3. WEC performance model verification progress report #2
4. Testing support progress report #2
5. WEC performance model verification final report

The present technical note refers to the *first* deliverable for this phase and documents the progress that has been made on the analysis of the first generic WEC model; *a rounded cylinder single-body point absorber*.

The *rounded cylinder single-body point absorber* is an example of one of the simplest type of WEC device and is therefore a good basis for primary verification of HNEI's own WEC performance model. The performance and the loads relating to a given device will depend on its size in respect to the range of sea conditions that it experiences at a given site. HNEI has expressed interest in understanding whether different optimum sizes of device can be chosen for different site locations (e.g. would a relatively small WEC be more most appropriate for the WETS site, where shorter energy periods are more frequent, as opposed to other more exposed locations) [4].

DNV GL has therefore agreed to undertake an investigation into WEC sizing in order to enlighten this issue and in order to select an appropriate scale of device upon which further verification exercises will be performed. Note that there are very many complex techno-economic factors that would feed into this decision for a WEC developer, which it will not be possible to explore within this project. However, some of the main principles in selecting an optimum size will be demonstrated here and the process may be extended by HNEI at their convenience in order to obtain a more comprehensive analysis. This technical note focuses on the baseline numerical modelling of the rounded cylinder device and the size selection methodology. Subsequent deliverables will then focus on the derivation of detailed results assuming the WEC size has been fixed.

DNV GL will generate a database of results that demonstrate the performance of the device for a range of scales. This will provide HNEI with a broad range of data for validation purposes and also allow for an investigation into whether optimum scales of device can be chosen for different site locations.

Section 3 and Section 4 of this technical note describes the WaveDyn model that has been created for the rounded cylinder single-body point absorber and the range of sea state simulations that have been run.

Section 5 provides a summary of the power performance for the WEC model for a range of device scales. The full set of detailed results are not provided with this current progress report, but will be supplied as part of subsequent deliverables, accompanied by analysis of the WEC behaviour.

In the final part of this technical note, an attempt is made to approximately identify an optimum scale in regard to *cost per MW of rated power output* for the generic device. Actual design optimization would be expected to be based on Levelized Cost of Energy (LCOE), including detailed analysis of various capital costs (e.g. WEC fabrication, foundation, installation etc.), operational costs and balance of plant costs. However, in the simplest case it is proposed that comparisons based on power output per unit structural mass can provide a useful basis for making relative comparisons of optimum scale for different site conditions.

Section 7 describes approximate calculations for the requirements of structural steel for the rounded cylinder float for the chosen generic WEC, based on currently available design standards. This information is used in section 5, together with the power performance data already described in section 6 to calculate the *cost per MW rated power* for a range of device scales at the Wave Energy Test Site (WETS) in Hawaii. Further to this, the same calculation is repeated for the European Marine Energy



Centre (EMEC) of the Orkney Islands in the UK in order to demonstrate the comparison of how optimum scale may differ for a more energetic site.

Any enquiries regarding this technical note should be addressed to:

John Roadnight

Email: john.roadnight@dnvgl.com

Tel: +44 (0) 203 816 5576

3 WEC DEFINITION

3.1 Overview of scaling methodology

The performance and loading relating to a device will depend on its size in respect to the range of sea conditions that it experiences at a given site. For a given WEC, a smaller scale of the device will tend to respond more actively to shorter period waves than a larger scale of the device.

The effect of scale could be investigated by creating and running separate WaveDyn models for each individual size of device. However, this would require the creation of separate hydrodynamic databases (see section 4.3) for each scale, which is a computationally expensive task and also requires the repetition of many WaveDyn simulations for each model.

An alternative approach is to use the concept of Froude scaling in order to allow the use of a single hydrodynamic database for all scales of device. The concept of scaling was described in section 6.5 of the Test Protocols Final report [16], in the previous phase of this project. For clarity, some of this detail is described again below.

Froude scaling is commonly used to infer the behaviour of a 'full-scale' device from tests with a scale prototype. In order to do this, it is desired that the device be in geometric, kinematic and dynamic similarity with the full-scale WEC. *Geometric* similarity requires that there is a fixed ratio of dimensions between the prototype and the full-scale device; *kinematic* similarity requires that there is a fixed ratio of velocities between the prototype and the full-scale device and *dynamic* similarity requires that there is a fixed ratio of forces between the prototype and the full-scale device. Due to the wide range of forces which act on a WEC, it is not possible to scale all of these at the same ratio. The approach taken in WEC testing is to use a scaling criterion which keeps the dominant forces acting on the WEC in a fixed ratio.

The motion of a WEC in ocean waves is primarily governed by gravitational and inertial forces. The ratio between inertial and gravitational forces is represented by the Froude number, F_n , given by:

$$F_n = \frac{U}{\sqrt{gL}} \quad (1)$$

where U and L (in this subsection only) are representative velocity and length scales respectively, and g is the modulus of the acceleration due to gravity. Froude scaling can be described as the set of laws which maintain the same Froude number at model scale and full-scale.

Under Froude scaling all lengths (e.g. WEC geometry, water depth, wave height, wavelength, etc.) are scaled by the same factor k . Scaling factors for other quantities calculated from (1) are presented in Table 3.1.

Quantity	Scaling
Wave height and length	k
Wave period	$k^{0.5}$
Wave frequency	$k^{-0.5}$
Power density	$k^{2.5}$
Linear displacement	k
Angular displacement	1
Linear velocity	$k^{0.5}$
Angular velocity	$k^{-0.5}$
Linear acceleration	1
Angular acceleration	k^{-1}
Mass	k^3
Force	k^3
Torque	k^4
Power	$k^{3.5}$
Linear stiffness	k^2
Angular stiffness	k^4
Linear damping	$k^{2.5}$
Angular damping	$k^{4.5}$

Table 3.1 Froude Scaling rules

Froude scaling laws are valid when gravitational and inertial forces are dominant and viscous forces can be disregarded. Froude scaling does not maintain the correct ratio between inertial and viscous forces. To maintain this ratio at partial scale the Reynolds number, Re , would need to be the same, where

$$Re = \frac{UL}{\nu} \quad (2)$$

and ν is the kinematic viscosity of the fluid. Since the kinematic viscosity is a property of the fluid and the ratio between U and L is determined by the Froude number, it is not possible to simultaneously maintain the same Froude and Reynolds numbers at partial scale. This means that viscous effects, such as vortex shedding and drag, may not be correctly scaled. Such effects may be more significant at reduced scale (e.g. viscous damping on the hull and mooring lines will be greater at model scale than at full-scale). However since gravitational forces normally have the dominant effect on WEC motion, Froude scaling is typically used for WEC modelling.

Other viscous properties include surface tension effects. These are generally considered negligible for wavelengths greater than 0.1m (a period of about 0.25 seconds in deep water) and so their effect on full scale devices at sea can be neglected.

In regard to the current project, the intention is to generate a database of hydrodynamics terms and for a single scale of the chosen generic single body point-absorber WEC (see following sections). A single WaveDyn model will then be run for a large range of irregular sea states to generate tables of results (e.g. power output, kinematics, forces). Following this, the Froude scaling rules listed in Table 3.1 will be applied to the 'model scale' results to produce equivalent results for a range of other scales of the device.

3.2 Definition of the generic single body point absorber

The chosen generic WEC is based on the rounded cylinder single-body point absorber that has previously been experimented upon in a wave tank [6]. This is a single taut-moored floating wave energy converter.

As described above, a single scale of the WEC device will be modelled in WaveDyn and then results will be scaled using Froude scaling rules to generate equivalent results for different sizes of device. The model scale device used for tank testing is therefore described here.

As shown in Figure 3-1, the modelled floating body consisting of a 0.5 m diameter hemisphere and a 0.5 m diameter, 0.25 m high closed cylinder. The total dry mass of the model is 43.2 kg. The centre of mass is 0.319 m from the top of the cylinder (on the central axis). The inertia matrix is defined as:

$$I_{xx} = I_{yy} = 1.59 \text{ kg/m}^2 \quad I_{zz} = 1.25 \text{ kg/m}^2 \quad I_{xy} = I_{xz} = I_{yz} = 0.$$

The PTO is idealised as consisting of a linear spring and linear damper:

- Linear spring constant, $k = 66.3 \text{ N/m}$. The unloaded length of the spring is 0.36m. When the buoy is stationary and attached to the mooring, the spring is extended by 0.54m, resulting in a mooring 'pre-load' force of 35.8N.
- Linear damping coefficient, $C = 37.7 \text{ Ns/m}$ (see section 3.3). Note that damping was not present in the device tested in [6].

The mooring line is taken to be a tether, 1.337m long with a spring constant of 35000 N/m.

The PTO is attached to a pivot at a height of 0.25m above the tank floor. The water depth is set at 2.8m.

The pre-load in the mooring line results in an increase in the draft from 0.303 m in the free-floating case, to 0.322m draft in the moored case (corresponding to a displaced mass of water of 46.85kg¹).

The spring constant of the combined components (PTO spring and tether) can be calculated as:

$$\frac{1}{k_{total}} = \frac{1}{k_1} + \frac{1}{k_2}$$

where k_{total} is the spring constant of the combined components, and k_1 and k_2 are the spring constants of each component. The overall spring coefficient k_{total} is 66.17kNm, which is only 0.2% different from the 66.3kNm PTO spring constant, so the tether is considered rigid in the numerical model.

It is assumed that the imposed preload in the mooring avoids any slackening of the tether. For this to be valid it is necessary that any negative heave motion of the buoy during operational seas does not exceed the initial spring extension. As an example, for a device scale of $k=20$ the equivalent initial spring extension will be $0.54\text{m} \cdot 20 = 10.8\text{m}$.

¹ Note that the original WAMIT calculation for the hydrodynamic database was run based on a buoy draft of 0.313m rather than 0.322m. The 3% difference in draft is not expected to have significant effect on the calculation of the hydrodynamic terms or hydrostatic stiffness.

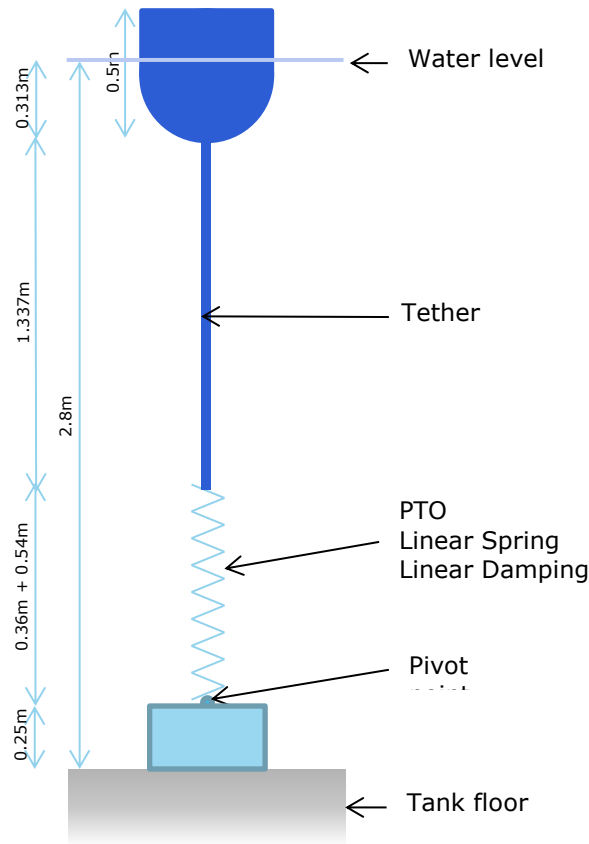


Figure 3-1 Schematic diagram of the generic WEC device moored to the tank floor.

3.3 PTO damping

For a single body point absorber operating in the heave mode with constant linear PTO damping γ_d , power capture will be optimised for a chosen wave frequency ω_0 when 'real' tuning of the damping is achieved (5.27 of [22]):

$$\gamma_d = \sqrt{[b_{33}(\omega_0)]^2 + \omega_0^2 \left[M + m_{33}(\omega_0) - \frac{K_{33}}{\omega_0^2} \right]^2} \quad (3)$$

where

$b_{33}(\omega_0)$ is the hydrodynamic radiation damping in heave due to heave motion for the buoy at frequency ω_0

M is the structural mass of the buoy

$m_{33}(\omega_0)$ is the hydrodynamic added mass of the buoy in heave due to heave motion at frequency ω_0

K_{33} is the stiffness (hydrostatic and mooring) in heave

In reality a WEC will experience a variety of irregular seas, each composed of a spectrum of frequencies. Therefore, without advanced control methodologies it is not possible to concurrently optimise power capture for all wave components. For the present case, a single constant value of PTO damping will be therefore be chosen. This is taken to be the optimal damping value at a frequency where the device is likely to perform well (the resonant frequency of the undamped device).

The following method has been followed to approximately define the PTO damping on the resonant frequency for the model scale device.

1. A version of the WaveDyn model described in section 3.1 above is first run with zero PTO damping for a series of regular waves in order to generate an response amplitude operator (RAO) curve for heave motion. This RAO is shown in Figure 3-2.
2. The frequency for calculating PTO damping is chosen to equal the frequency of the peak of the heave displacement RAO. i.e. $\omega_0 = 5.8 \text{ rad/s}$. This equates to a period of $T = \frac{2\pi}{5.8} = 1.08 \text{ s}$
3. The hydrodynamic radiation damping $b_{33}(\omega_0)$ and added mass $m_{33}(\omega_0)$ are extracted from the curves shown in Figure 4-4 and Figure 4-5. i.e. $b_{33}(5.8 \text{ rad/s}) = 35.2 \text{ Ns/m}$ and $m_{33}(5.8 \text{ rad/s}) = 14.7 \text{ kg}$
4. A PTO damping coefficient is then calculated using equation (3)

$$\gamma_d = 37.7 \text{ Ns/m},$$

where the structural mass of the buoy $M = 43.2 \text{ kg}$, and the stiffness $K_{33} = 1926.2 \text{ N/m} + 66.3 \text{ N/m}$.

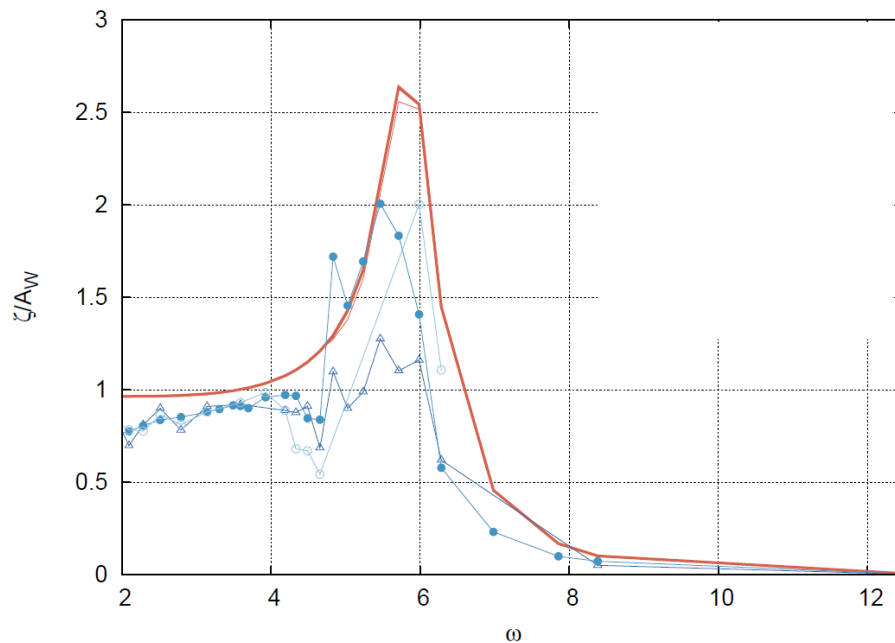


Figure 3-2 RAO of single point absorber in heave (bold red line shows RAO for the WaveDyn model with zero PTO damping)

It is noted that inclusion of PTO damping will influence the response of the WEC model. Therefore the peak of the actual heave displacement RAO curve after inclusion of PTO damping will differ slightly from the 5.8 rad/s value identified above. However, it is considered only necessary to obtain an approximate estimate the resonant frequency for picking a level for PTO damping as verification may be performed on the results whether or not the set-up is optimal.

3.4 Scaling range

The WaveDyn model described above has a floater diameter of $D=0.5 \text{ m}$ and overall height $H=0.5 \text{ m}$ and represents a scale of device suited only to tank tests and not open ocean conditions.

A range of scales from $k=5$ to 80 will therefore be considered, which equates to a range of floater diameters from $D=2.5 \text{ m}$ to 40 m . It is recognised that 40 m diameter is at the very extreme end of likely



WEC sizes. As noted in section 3.1, other physical properties of the WEC will scale following the rules given in Table 3.1. For example, mooring line stiffness will scale with k^2 and PTO linear damping will scale with $k^{2.5}$.

4 WAVEDYN MODEL

WaveDyn is a multi-body, time-domain, simulation tool developed specifically for evaluating WEC performance and loading. The software allows a user to construct a numerical representation of a WEC by connecting structural, hydrodynamic, power take-off (PTO) and moorings components using a flexible user interface. Control actions may be implemented through the PTO components, and simulations may be run with regular or irregular input sea states, for multiple wave directions.

In the WaveDyn release used for the present study (version 1.2), the basic, linear radiation-diffraction hydrodynamics formulation may be supplemented with nonlinear calculation models for the incident wave Froude-Krylov force and the hydrostatic force. Viscous effects may be applied by specifying drag coefficients in WaveDyn (although in the current model, none is used). The hydrodynamics models are the focus of this study and so are described in more detail below. However, none of these aforementioned supplementary effects are considered in the present verification study.

4.1 Theory

The basic linear formulation, for a nominal rigid body able to move in a single degree of freedom, x may be written as:

$$(m_m + m_r(\infty))\ddot{x}(t) + f_{hs}(t) + \int_{-\infty}^t k(t - \tau)\dot{x}(\tau)d\tau = f_e(t) + f_{ext}(\dots) \quad (4)$$

where:

x	is the body displacement from its equilibrium position
m_m	is the physical body mass
m_r	is the added mass relating to the body radiation force at infinite wave frequency
$f_{hs}(x)$	is the hydrostatic (buoyancy force)
$\int_{-\infty}^t k(t - \tau)\dot{x}(\tau)d\tau$	is the radiation force convolution term based on the body impulse response function, $k(t)$ and the body velocities.
$f_e(t)$	is the excitation force due to the incident waves
$f_{ext}(x, \dot{x}, \dots, t)$	represents all additional, non-hydrodynamic applied forces such as those due to the moorings system, the turbine itself and structural dynamics effects.

The hydrodynamic forcing terms rely on properties computed for the body geometry by an external flow solver (e.g. WADAM or WAMIT). WaveDyn uses this information (excitation force coefficients, added mass, radiation damping) to synthesise matrices of time-domain hydrodynamic forces to apply to the multi-body structural model of the device.

The time-domain excitation force expression can be obtained as the superposition of the force contributions from each of the wave frequencies in the incident wave train (which is compiled as the linear superposition of n sinusoidal, regular wave components, each with a phase ϕ_n):

$$f_e = \sum_n f_{e,n} = \sum_n \text{Re}(\mathbb{F}_{e,n} e^{j(\omega t + \phi_n)}) \quad (5)$$

The radiation force component is directly dependant on the system response (which may be non-linear as a result of the structural or PTO models being used). In WaveDyn, the force is computed as a time domain manifestation of a frequency dependent impedance term:

$$f_r(\omega) = G(\omega)U(\omega) = (j\omega m_r(\omega) + B_r(\omega))U(\omega) \quad (6)$$

The added mass is isolated in the conversion to the time domain formulation:

$$f_r(t) = m_r(\infty)\ddot{x} + \int_{-\infty}^t k(t-\tau)\dot{x}(\tau)d\tau \quad (7)$$

Where the impulse response function, $k(t)$ is defined by the inverse transform:

$$k(t) = \frac{2}{\pi} \int_{-\infty}^{\infty} B_r(\omega) \cos(\omega t) d\omega \quad (8)$$

The hydrostatic force, $f_{hs}(x)$, incorporates all buoyancy related effects and is applied to each body as a combination of a constant, mean buoyancy, $\overline{f_{hs}}$ acting upwards through a fixed centre of gravity and a hydrostatic stiffness K_{hs} that incorporates a linearization of the variation in the wetted surface area as the body moves relative to the mean waterline.

$$f_{hs}(t) = \overline{f_{hs}} + K_{hs}x(t) \quad (9)$$

All weight related terms are included directly in the structural model and so the hydrostatic stiffness matrix used by WaveDyn does not include these.

4.2 Structural Model

A block diagram shown in Figure 4-1 represents the multi-body structure of the WEC model in WaveDyn. In the structural model, the buoy is represented as a rigid body with mass, inertia and hydrodynamic properties. It is connected to the ground element through a hinge rotating joint, only free in pitch, and a spring sliding joint, to which the mooring stiffness properties are assigned. The component connectivity is defined using a series of nodes and mass-less rigid links, used to specify the distance between the rigid body centres of mass and PTO pivot locations. The dimensions, masses and inertial properties of the WEC are summarised in Table 4.1, whilst a more complete description of each component in the model is provided below.

The 'Ground' is the starting point, in global space, from which the structural connectivity is defined. Its location is typically set to $\{0\}\{0\}\{0\}$, which places the Ground and global coordinate system origin in the same physical location.

'RigidLink0' is the physical, completely rigid, but massless connection that represents the space between the seabed and the pivot point. Its distal node offset is set to 0.25m (the height of the pivot point).

'Hinge11' represents the pivot point. It is only allowed to pitch (for symmetry reasons in the unidirectional waves considered in this technical note).

'RigidLink1' represents the space occupied by the spring. The distal node offset is set to 0.8987m in the moored configuration (spring free length plus spring extension), and to 0.9080m in the unmoored configuration (distance between Node N3, bottom of the tether, and Node N1, top of the pivot point).

The 'Spring' body is a sliding joint that is allowed to heave, and a linear stiffness PTO component. The stiffness is set to 66.3N/m as described in section 3 above.

'RigidLink2' represents the tether, considered as rigid. The distal node offset is set to 1.337m (calculated as the difference between the water depth and the sum of the buoy draft, the spring length and the pivot height).

'Hinge 21' represents the attachment point of the mooring at the bottom of the hemisphere. It is only allowed to pitch (for symmetry reasons in unidirectional waves).

'RigidLink3' represents the space between the bottom of the hemisphere and the centre of mass of the buoy. Its distal node offset is set to 0.181m.

Finally, the rigid body 'Buoy' is a point mass which experiences linear and nonlinear inertial and weight forces. It is accompanied by hydrodynamic and hydrostatic properties imported from the WAMIT. The WAMIT simulation set up is described in in Section 4.3.

Mass (kg)	43.2			
Displaced mass - in still water (kg)	46.85			
Height of buoy (m)	0.5			
Diameter of buoy (m)	0.5			
Inertia tensor about centre of mass (kg.m ²)	1.59	0	0	
	0	1.59	0	
	0	0	1.25	

Table 4.1 Physical properties of the WEC buoy, as defined in WaveDyn

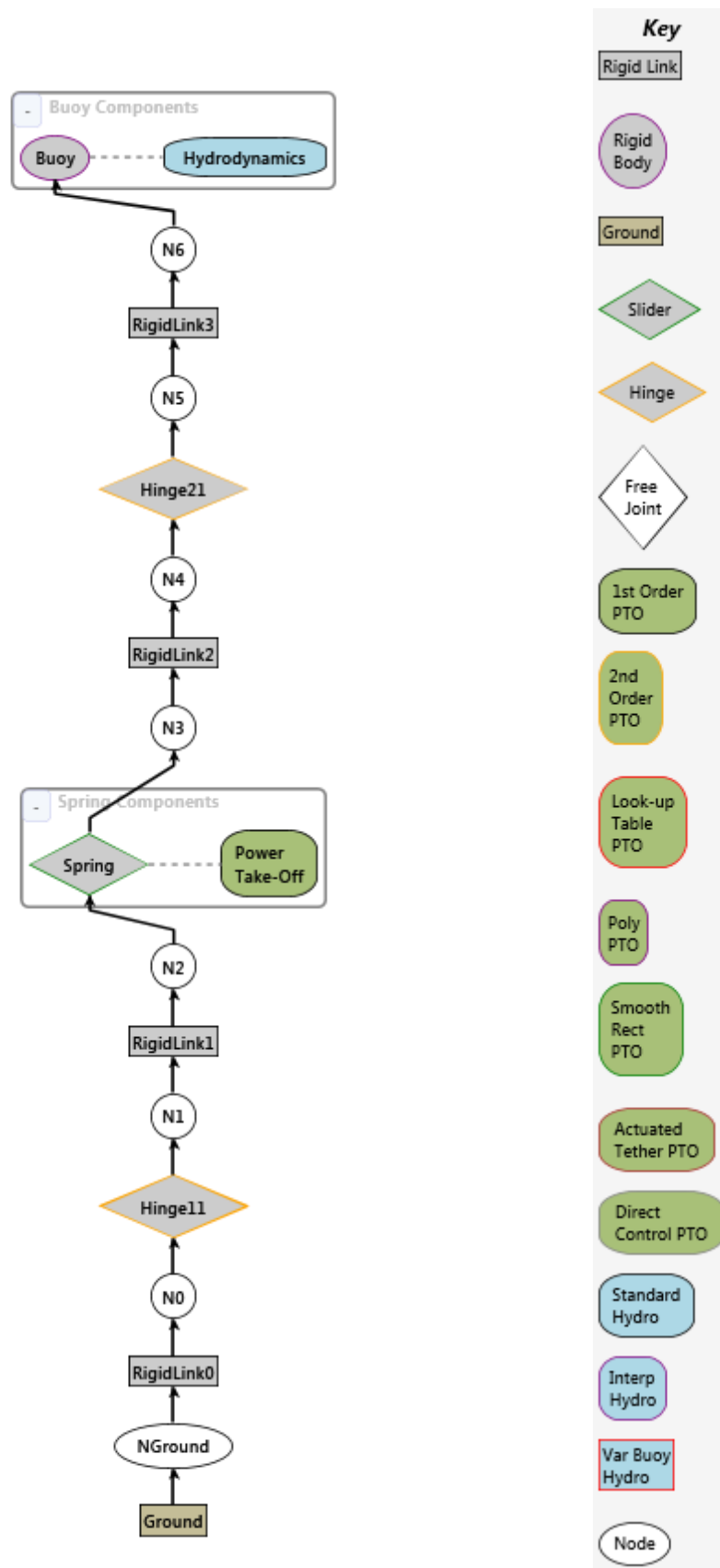


Figure 4-1 WaveDyn model schematic.

4.3 Hydrodynamic Model

The linear hydrodynamic coefficients associated with the buoy were obtained from WAMIT. The geometry was defined using the MultiSurf CAD package. 'High-order' geometry definition files (where the surface is represented by curved splines) were created, allowing a faster and more accurate simulation than would be possible using a low order, flat quadrilateral panel method. A mesh refinement study was completed to ensure all relevant hydrodynamic properties had converged.

Figure 4-2 presents the MultiSurf mesh of the buoy as viewed in WaveDyn. Only the wetted surface at equilibrium is meshed.

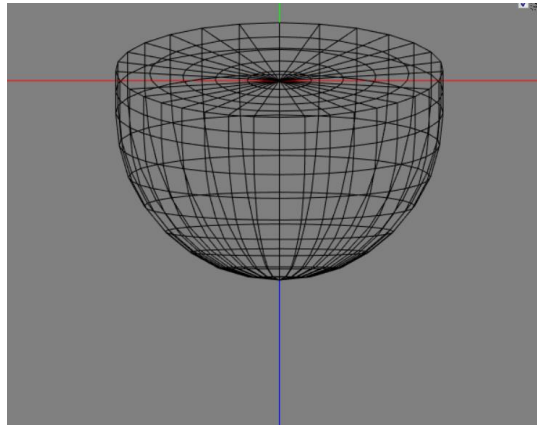


Figure 4-2 View of the buoy mesh used in the WAMIT calculations.

Hydrodynamic coefficients were calculated for 294 incident wave frequencies and 24 directions. The WAMIT hydrodynamic data have been imported in WaveDyn as part of the hydrodynamic definition of the buoy. Impulse response functions with a length of 9s were calculated as part of the import process and were found to be of sufficient length to satisfactorily complete the radiation force convolution integral (the impulse response decayed to zero within 9s for all freedoms).

The excitation force amplitude and radiation damping for the buoy are plotted in Figure 4-3 and Figure 4-6 respectively.

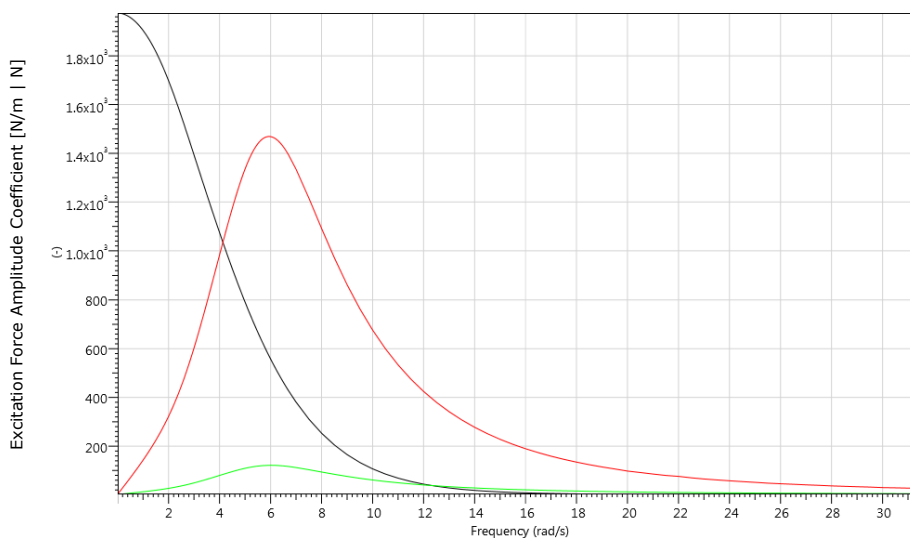


Figure 4-3 Buoy excitation force coefficient for Heave (black), Pitch (red) and Surge (green)

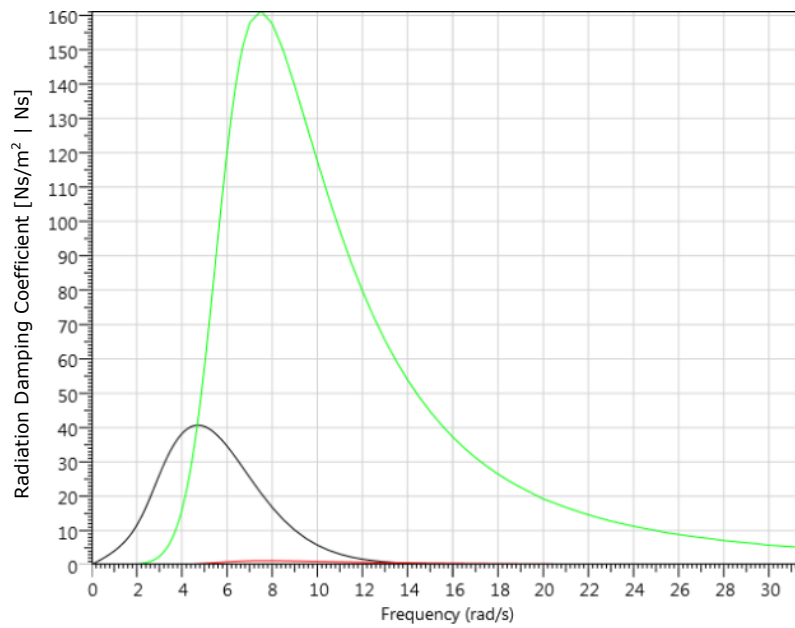


Figure 4-4 Buoy radiation damping in Heave (black), Pitch (red) and Surge (green)

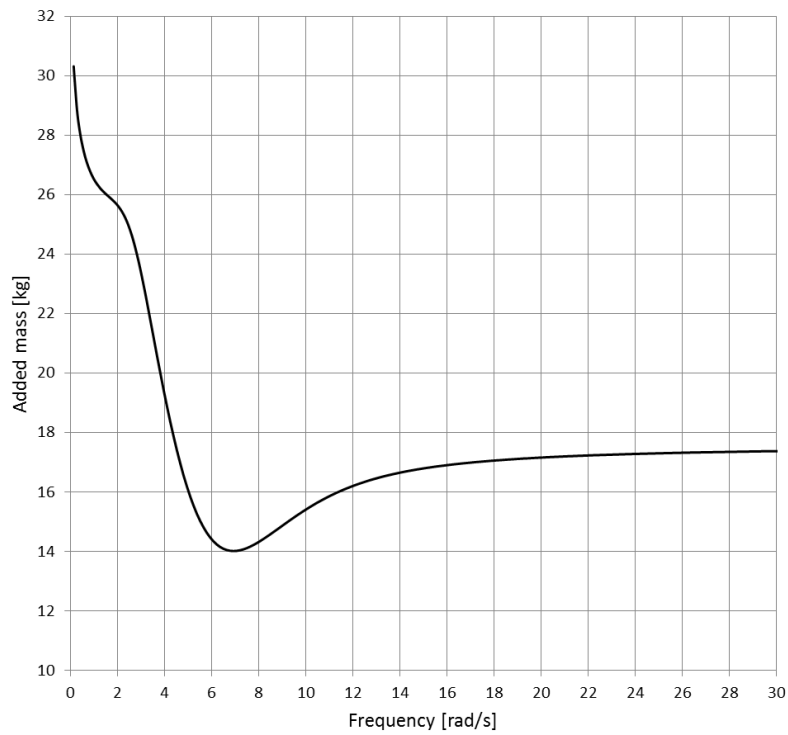


Figure 4-5 Buoy added mass in Heave

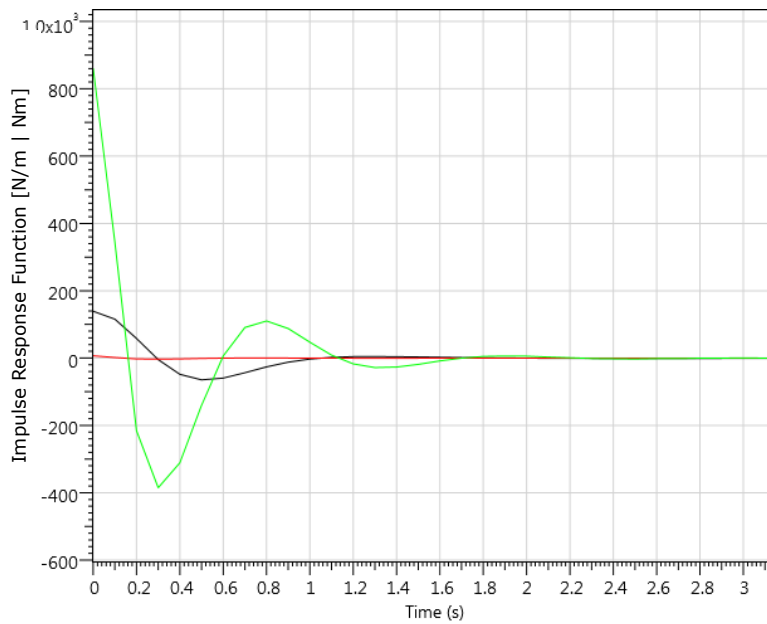


Figure 4-6 Impulse response functions for Heave (black), Pitch (red) and Surge (green)

4.4 Sea states

Scatter tables of occurrence for significant wave height, H_s and energy period, T_e are shown below in Table 4.2 and Table 4.3 respectively for Wave Energy Test Site (WETS) in Hawaii and the European Marine Energy Centre (EMEC) of the Orkney Islands in the UK. The occurrence data for the WETS site is extracted from Table 2 of the Hawaii Wave Energy characterisation report [7] and the scatter table for the EMEC site is based on data described in [8].

It can be seen that the range of non-negligible occurrence for the two sites falls between $T_e=2s$ to $17s$ and $H_s=0.5m$ to $7.5m$.

		Energy Period, T_e [sec]																
		1	2	3	4	5	6	7	8	9	10	11	12	13	14	15	16	17
Significant Wave Height, H_s [m]	5.5	0.0%	0.0%	0.0%	0.0%	0.0%	0.0%	0.0%	0.0%	0.0%	0.0%	0.0%	0.0%	0.0%	0.0%	0.0%	0.0%	0.0%
	5	0.0%	0.0%	0.0%	0.0%	0.0%	0.0%	0.0%	0.0%	0.0%	0.0%	0.0%	0.0%	0.0%	0.0%	0.0%	0.0%	0.0%
	4.5	0.0%	0.0%	0.0%	0.0%	0.0%	0.0%	0.0%	0.0%	0.1%	0.0%	0.0%	0.0%	0.0%	0.0%	0.0%	0.0%	0.0%
	4	0.0%	0.0%	0.0%	0.0%	0.0%	0.0%	0.0%	0.1%	0.2%	0.1%	0.0%	0.0%	0.0%	0.0%	0.0%	0.0%	0.0%
	3.5	0.0%	0.0%	0.0%	0.0%	0.0%	0.0%	0.0%	0.5%	0.4%	0.1%	0.1%	0.1%	0.0%	0.0%	0.0%	0.0%	0.0%
	3	0.0%	0.0%	0.0%	0.0%	0.0%	0.0%	0.3%	1.8%	0.7%	0.5%	0.3%	0.3%	0.1%	0.1%	0.0%	0.0%	0.0%
	2.5	0.0%	0.0%	0.0%	0.0%	0.0%	0.0%	2.7%	3.0%	1.5%	1.0%	0.7%	0.5%	0.2%	0.1%	0.0%	0.0%	0.0%
	2	0.0%	0.0%	0.0%	0.0%	0.0%	2.0%	9.7%	5.3%	3.3%	2.0%	1.4%	0.9%	0.4%	0.2%	0.1%	0.0%	0.0%
	1.5	0.0%	0.0%	0.0%	0.0%	0.1%	10.1%	12.5%	6.9%	4.8%	3.2%	2.2%	0.9%	0.3%	0.1%	0.0%	0.0%	0.0%
	1	0.0%	0.0%	0.0%	0.0%	0.4%	3.6%	4.5%	3.6%	2.5%	1.5%	0.8%	0.2%	0.1%	0.0%	0.0%	0.0%	0.0%
0.5	0.0%	0.0%	0.0%	0.0%	0.0%	0.1%	0.1%	0.1%	0.0%	0.0%	0.0%	0.0%	0.0%	0.0%	0.0%	0.0%	0.0%	

Table 4.2 Scatter table of occurrence for WETS site

		Energy Period, T_e [sec]																
		1	2	3	4	5	6	7	8	9	10	11	12	13	14	15	16	17
Significant Wave Height, H_s [m]	8	0.0%	0.0%	0.0%	0.0%	0.0%	0.0%	0.0%	0.0%	0.0%	0.0%	0.0%	0.0%	0.0%	0.0%	0.0%	0.0%	0.0%
	7.5	0.0%	0.0%	0.0%	0.0%	0.0%	0.0%	0.0%	0.0%	0.0%	0.0%	0.1%	0.1%	0.1%	0.0%	0.0%	0.0%	0.0%
	7	0.0%	0.0%	0.0%	0.0%	0.0%	0.0%	0.0%	0.0%	0.0%	0.0%	0.1%	0.1%	0.1%	0.0%	0.0%	0.0%	0.0%
	6.5	0.0%	0.0%	0.0%	0.0%	0.0%	0.0%	0.0%	0.0%	0.0%	0.1%	0.1%	0.1%	0.1%	0.1%	0.0%	0.0%	0.0%
	6	0.0%	0.0%	0.0%	0.0%	0.0%	0.0%	0.0%	0.0%	0.1%	0.2%	0.2%	0.3%	0.1%	0.0%	0.0%	0.0%	0.0%
	5.5	0.0%	0.0%	0.0%	0.0%	0.0%	0.0%	0.0%	0.0%	0.0%	0.2%	0.3%	0.2%	0.2%	0.1%	0.0%	0.0%	0.0%
	5	0.0%	0.0%	0.0%	0.0%	0.0%	0.0%	0.0%	0.2%	0.5%	0.4%	0.3%	0.3%	0.2%	0.1%	0.0%	0.0%	0.0%
	4.5	0.0%	0.0%	0.0%	0.0%	0.0%	0.0%	0.0%	0.3%	0.6%	0.5%	0.6%	0.5%	0.2%	0.1%	0.0%	0.0%	0.0%
	4	0.0%	0.0%	0.0%	0.0%	0.0%	0.0%	0.2%	0.6%	0.8%	0.7%	0.8%	0.6%	0.2%	0.1%	0.0%	0.0%	0.0%
	3.5	0.0%	0.0%	0.0%	0.0%	0.0%	0.1%	0.6%	0.7%	0.9%	1.1%	1.1%	0.7%	0.2%	0.1%	0.0%	0.0%	0.0%
	3	0.0%	0.0%	0.0%	0.0%	0.0%	0.4%	0.8%	0.9%	1.4%	1.7%	1.3%	0.8%	0.2%	0.1%	0.0%	0.0%	0.0%
	2.5	0.0%	0.0%	0.0%	0.0%	0.1%	0.9%	0.8%	1.7%	2.6%	2.3%	1.5%	0.8%	0.3%	0.1%	0.0%	0.0%	0.0%
	2	0.0%	0.0%	0.0%	0.1%	0.6%	1.0%	1.3%	2.5%	3.4%	2.7%	1.6%	0.8%	0.4%	0.2%	0.1%	0.0%	0.0%
	1.5	0.0%	0.0%	0.1%	0.6%	0.8%	1.1%	2.4%	4.5%	3.7%	2.2%	1.2%	0.6%	0.3%	0.1%	0.1%	0.0%	0.0%
	1	0.0%	0.0%	1.1%	0.6%	0.8%	2.0%	4.1%	5.0%	3.2%	1.7%	1.0%	0.5%	0.2%	0.1%	0.0%	0.0%	0.0%
0.5	0.0%	0.5%	0.5%	0.2%	0.7%	1.7%	2.4%	2.1%	1.4%	0.6%	0.3%	0.2%	0.1%	0.1%	0.0%	0.0%	0.0%	

Table 4.3 Scatter table of occurrence for EMEC site

It is necessary to choose a suitably broad range of irregular seastates to run at model scale, such that, after scaling for all chosen scales of device ($k=5$ to 80), the scaled H_s and T_e values for each sea state will always encompass the chosen ranges of $T_e=2s$ to $17s$ and $H_s=0.5m$ to $7.5m$.

From Table 3.1, wave period scales with $k^{0.5}$ and wave height scales linearly with k .

Table 4.4 describes the choice of limiting values for the sea state parameters and Table 4.5 illustrates the chosen values of H_s and T_e in a scatter table format. The bold border lines indicate the extent of the EMEC sea state scatter table for the chosen largest and smallest scale devices.

The significant wave height H_s bins range from 0.005m to 1.939m at model scale. A non-uniform spacing between bins has been chosen in order to ensure that whatever scale is used, the resulting full-scale scatter table always has the same resolution around the $H_s=2m$, $T_e=10s$ point. The spacing between H_s bins increases with an increment factor of 1.25 (e.g. $1.939/1.551=1.25$). It should be noted that uniform spacing of bins is not necessary because an interpolation procedure is used in the post-processing of results described in section 5.

The energy period bins range from 0.223s to 8.4s at model scale. The spacing between T_e bins increases with an increment factor of 1.1 (e.g. $8.363/7.603=1.1$)

In total Table 4.5 represents 1200 simulations. SEA files were created for each of the 1200 cases, assuming unidirectional JONSWAP spectra with the defined significant wave height H_s and energy period

T_e for each case, and with a peak enhancement factor $\gamma = 1$. It is noted that with an axisymmetric device and mostly linear system the power and the heave loads will be the same as for spread seas. The repeat time for each case was defined as 200 times the energy period (e.g. for $T_e=9s$ the repeat period would be 1800s, or 30mins).

The WaveDyn simulation was run for a duration equal to the SEA file repeat time in each case plus an initial ramp-up time of 50s. During the post-processing of results the simulations outputs are truncated to remove the section of data associated with the ramp-up time before calculation of statistical values.

	Scale rule	Required range for full scale devices	Equivalent range for model scale	
			$k=1/5$	$k=1/80$
Wave Height, H_s	k	0.5m to 8m	0.1m to 1.6m	0.0625m to 0.1
Energy Period, T_e	$k^{0.5}$	2s to 17s	0.894s to 7.6s	0.223 to 1.90s

Table 4.4 Selection of T_e and H_s ranges for sea state scatter table at model scale

			Energy Period, Te																																						
			2.0	2.2	2.4	2.7	2.9	3.2	3.5	3.9	4.3	4.7	5.2	5.7	6.3	6.9	7.6	8.4	9.2	10.1	11.1	12.2	13.5	14.8	16.3	17.9	19.7	21.7	23.8	26.2	28.8	31.7	34.9	38.4	42.2	46.5	51.1	56.2	61.8	68.0	74.8
			0.5	0.6	0.6	0.7	0.7	0.8	0.9	1.0	1.1	1.2	1.3	1.4	1.6	1.7	1.9	2.1	2.3	2.5	2.8	3.1	3.4	3.7	4.1	4.5	4.9	5.4	6.0	6.6	7.2	7.9	8.7	9.6	10.6	11.6	12.8	14.1	15.5	17.0	18.7
			0.2	0.2	0.3	0.3	0.3	0.4	0.4	0.4	0.5	0.5	0.6	0.6	0.7	0.8	0.8	0.9	1.0	1.1	1.2	1.4	1.5	1.7	1.8	2.0	2.2	2.4	2.7	2.9	3.2	3.5	3.9	4.3	4.7	5.2	5.7	6.3	6.9	7.6	8.4
Largest scale	Smallest scale	Model scale																																							
155.10	9.69	1.939																																							
124.08	7.75	1.551																																							
99.26	6.20	1.241																																							
79.41	4.96	0.993																																							
63.53	3.97	0.794																																							
50.82	3.18	0.635																																							
40.66	2.54	0.508																																							
32.53	2.03	0.407																																							
26.02	1.63	0.325																																							
20.82	1.30	0.260																																							
16.65	1.04	0.208																																							
13.32	0.83	0.167																																							
10.66	0.67	0.133																																							
8.53	0.53	0.107																																							
6.82	0.43	0.085																																							
5.46	0.34	0.068																																							
4.37	0.27	0.055																																							
3.49	0.22	0.044																																							
2.79	0.17	0.035																																							
2.24	0.14	0.028																																							
1.79	0.11	0.022																																							
1.43	0.09	0.018																																							
1.14	0.07	0.014																																							
0.92	0.06	0.011																																							
0.73	0.05	0.009																																							
0.59	0.04	0.007																																							
0.47	0.03	0.006																																							
0.38	0.02	0.005																																							

Table 4.5 Scatter table showing full range of irregular sea states run on WaveDyn model

5 POST PROCESSING FOR WEC PERFORMANCE

Time-averaged PTO power absorbed P_i is extracted from the model scale WaveDyn time history results for each of the 1200 simulations shown in Table 4.5 and placed in a table with T_e and H_s ordinates.

For each scale of WEC device, a new power matrix is calculated by factoring this large power matrix using the following rule from Table 3.1.

$$P_{i,k} = P_i \cdot k^{3.5} \quad (10)$$

The energy period and significant wave height bin center values also have to be adjusted for the new scale of device by scaling the model scale bins.

$$T_{e,k} = T_e \cdot k^{0.5} \quad (11)$$

$$H_{s,k} = H_s \cdot k \quad (12)$$

For each scale of device we are only interested in a sub-section of the 1200 element power matrix that matches the ranges of the sea-state occurrence scatter tables for the WETS and EMEC sites described in Table 4.2 and Table 4.3.

The required format for this power matrix is shown in Table 5.1. This has 64 elements.

		Energy Period, T_e [sec]															
		2	3	4	5	6	7	8	9	10	11	12	13	14	15	16	17
Significant Wave Height, H_s [m]	8																
	7.5																
	7																
	6.5																
	6																
	5.5																
	5																
	4.5																
	4																
	3.5																
	3																
	2.5																
	2																
	1.5																
	1																
	0.5																

Table 5.1 Required of scatter table for the device scale power matrices

A new 64 element power matrix can be generated by interpolation of the appropriate 1200 element power matrix for each scale. However it is more accurate to carry out the interpolation based on *capture length*, which shows less variation with H_s and T_e than *power*. [9]

The concept of capture length was introduced in section 6.3 of the Test Protocols Final report [16], in the previous phase of this project.

The capture length for each bin is given by

$$L_i = \frac{P_i}{J_i} \quad (13)$$

An approximation for wave energy flux per unit width, J in deep water is given by

$$J = \frac{\rho g^2}{64\pi} H_s^2 T_e \quad (14)$$

Where H_s is significant wave height, T_e is the energy period and $\rho = 1025 \text{ kg/m}^3$, $g = 9.81 \text{ m/s}^2$

The deep water approximation is deemed sufficiently accurate for the WETS and EMEC sites which have water depths of 81m and 70m respectively.

A new 1200 element scatter table of *Wave energy flux per unit width J* is calculated for each scale of device. The resulting table is different for each scale due to the previous scaling of H_s and T_e bins using equation (11) and (12).

Following this, a 1200 element table of *capture length L* is calculated for each scale of device using equation (13).

Finally, a 64 element scatter table of *capture length L* is then calculated for each scale by interpolation of the appropriate 1200 capture length matrix, based on the H_s and T_e bins shown in Table 5.1. The annual average power for each scale of device is calculated by multiplying the relevant matrix of capture length L by the matrix of energy flux J and the occurrence data given in Table 4.2 and Table 4.3 for the two WETS and EMEC sites. i.e.

$$P_{avg} = \sum_{i=1}^{i=N} P_i \cdot f_i \quad (15)$$

Where $P_i = L_i \cdot J_i$ is the WEC output power per bin in the new scatter table and $f_i = \frac{n_i}{N}$ is the fraction of occurrence for each sea state bin and $\sum_{i=1}^{i=N} f_i = 1$

The Mean Annual Energy Production (MAEP) is defined as.

$$MAEP_{ALT} = T \cdot \sum_{i=1}^{i=N} P_i \cdot f_i \quad (16)$$

where T is the average length of a year which is 8766h.

6 WEC PERFORMANCE RESULTS

Figure 6-1 shows how the annual average power P_{avg} varies with scale of device for the WETS and EMEC sites. The absorbed WEC power is consistently higher for the EMEC site compared to WETS site. This is partially because the annual average energy flux per unit width J_{avg} , given by the following equation, is higher at the EMEC site.

$$J_{avg} = \sum_{i=1}^{i=N} J_i \cdot f_i \quad (17)$$

J_{avg} is found to be 13.86kW/m for the WETS site and 30.28kW/m for the EMEC site.

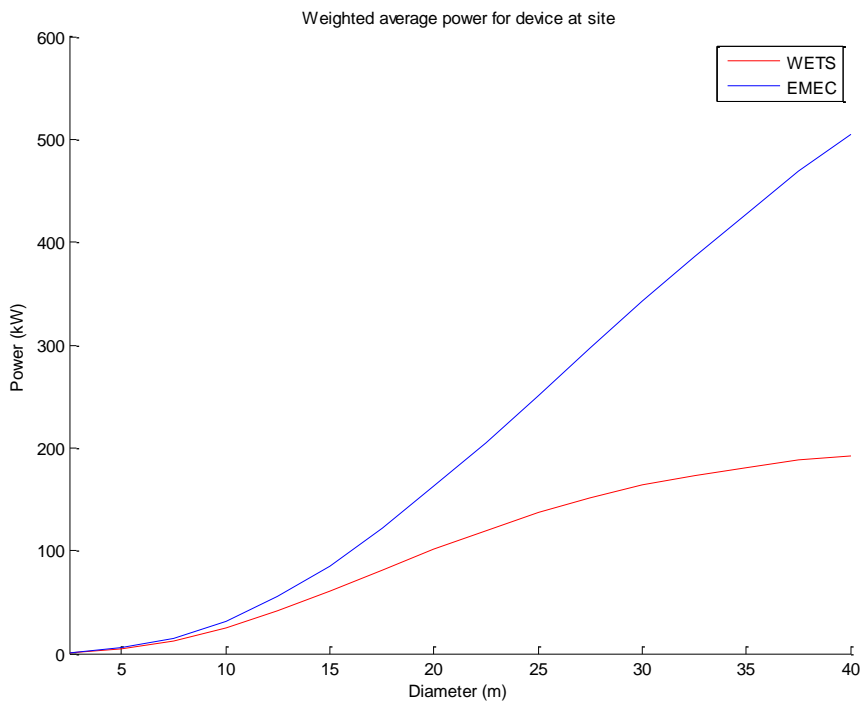


Figure 6-1 Annual mean power P_{avg} (kW) against WEC buoy diameter for WETS and EMEC sites

The annual average power P_{avg} is also shown in Figure 6-1 to increase with WEC size for both sites. This is partially because the wave resource (energy flux per unit width) for a given wave amplitude increases with wavelength and the larger diameter devices resonate at longer periods.

The calculated wave resource J is illustrated as a table in Figure 6-2 for the range of H_s and T_e bins under consideration. Figure 6-3 shows how the resonant period of the model-scale device (the period of peak RAO identified as 1.08s for the model scale device in section 3.3) scales with device size, using the scaling rule for period, $T_k = T \cdot k^{0.5}$.

Another important factor is whether the resonant response coincides with the most frequently occurring wave periods. As shown in equation (15), the annual mean power is the summation of the product of the of absorbed power P and the annual occurrence fraction f . Figure 6-4 and Figure 6-5 show scatter tables of the annual occurrence fraction f together with scatter tables of calculated WEC output power P for two sizes of device (5m and 20m) for the WETS and EMEC site. It can be seen that the peak of the power

matrix is well aligned with the peak in occurrence for the 20m diameter device, but less so for the 5m device. The peak occurrence is for an energy period of around 7 to 8s for the two sites, which is shown in Figure 6-3 to be the approximate resonant period for the 20m device.

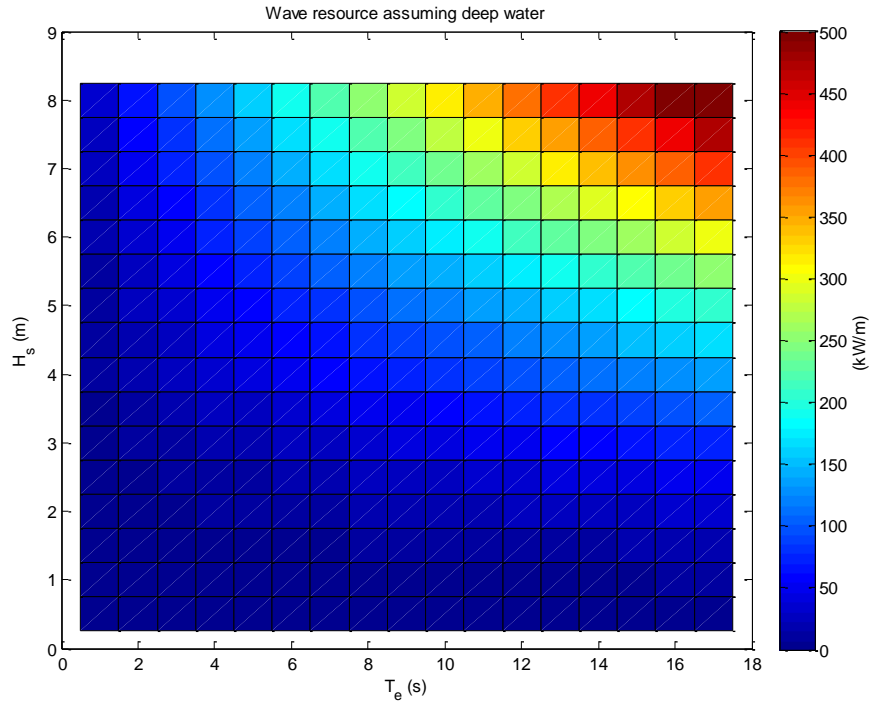


Figure 6-2 Wave energy flux per unit width J_t (kW/m) assuming deep water

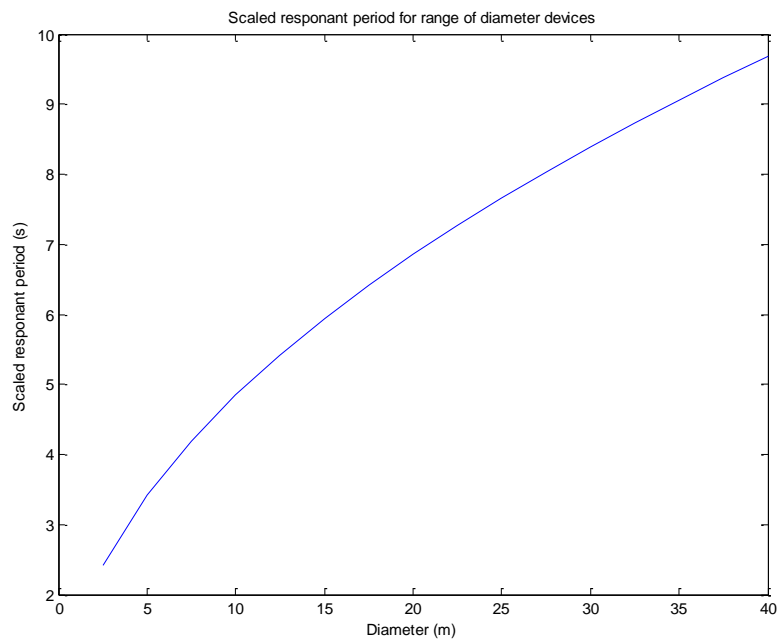


Figure 6-3 Scaled resonant period T (s)

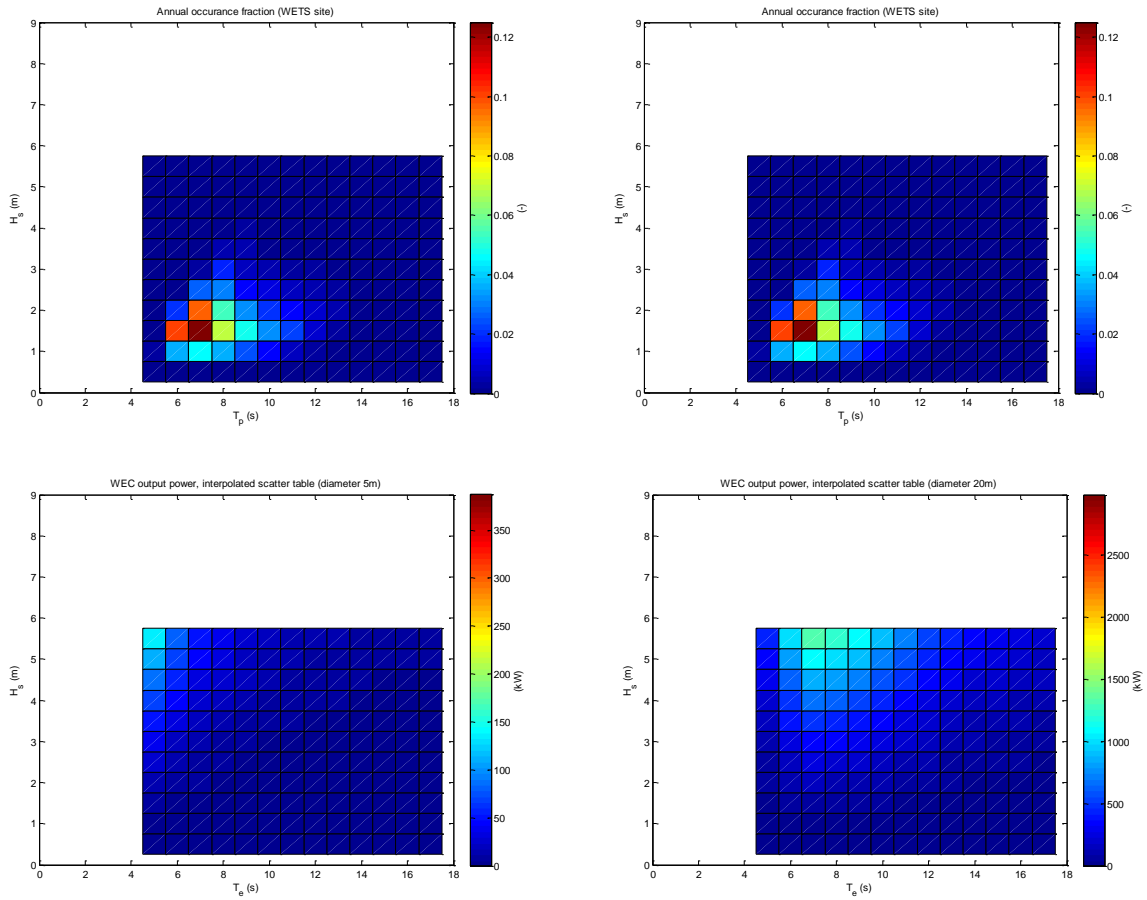


Figure 6-4 Top: Annual occurrence fraction f_i (-) WETS site, Bottom Left: Output power P_i (kW) for 5m diameter device, Bottom Right output power 20m diameter device

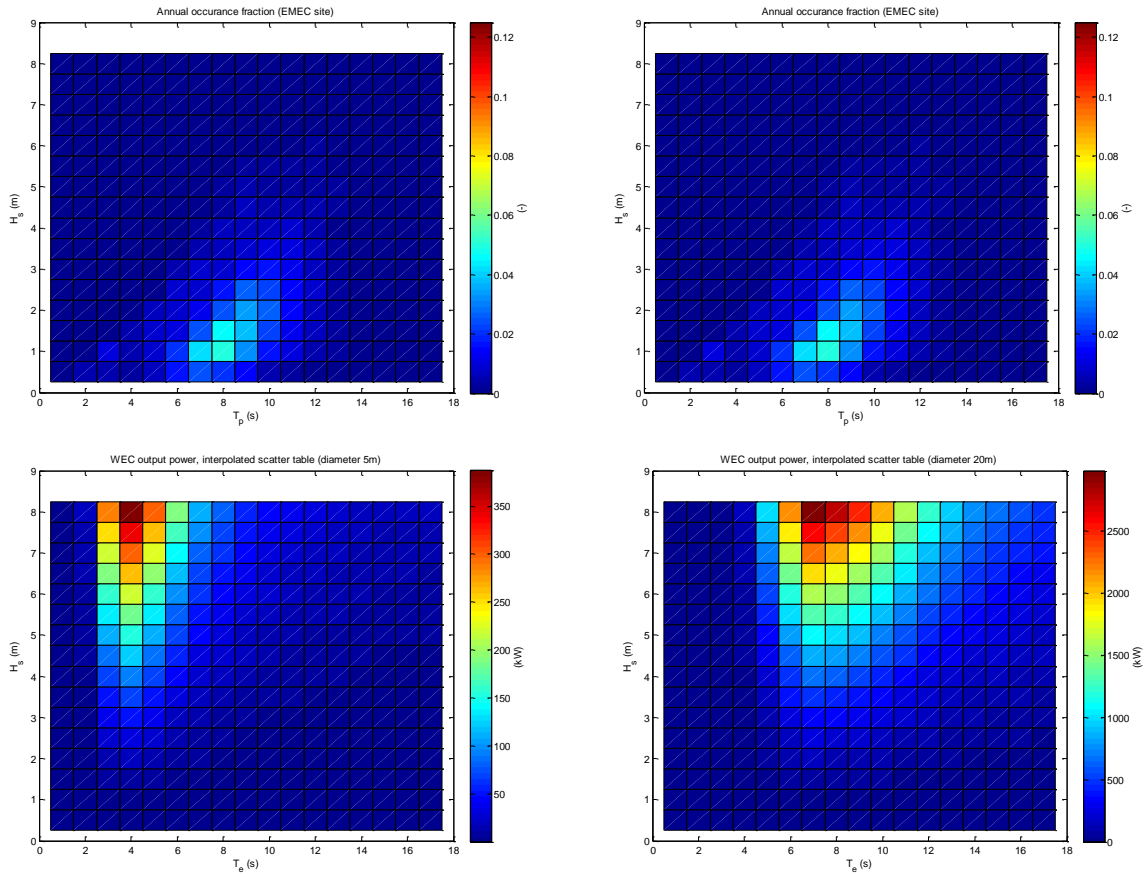


Figure 6-5 Top: Annual occurrence fraction f_i (-) EMEC site, Bottom Left: Output power P_i (kW) for 5m dia device, Bottom Right output power 20m dia device

7 CALCULATION OF STRUCTURAL MASS

The intention of this section is to demonstrate an approximate method for estimating the structural mass of the WEC float. The required thickness of plate is first calculated based on a design code approach for buckling strength criteria for a variety of scales of the device. The mass will then be calculated by multiplying this thickness by the surface area for the buoy at each scale.

7.1 Design loads

The plate thickness requirement will be estimated for a range of WEC float diameters from 10m to 80m following DNV GL offshore standards.

Structural loading is approximated using DNV-RP-C205 [11] and DNV-OS-E403 [10]. DNV-RP-C205 is used to make a check on wave slamming loads as described below.

DNV-OS-E403 provides guidance for design of offshore loading buoys which applies to floating (i.e. buoy) systems intended for loading/unloading of fluid cargoes such as crude oil, petroleum gas etc. into/from ships or other units in the open sea. Section 3.3 of the code provides simple relationships for calculating environmental loads in regard to hydrodynamic pressures acting on the main (weather) deck, sides and bottom of the buoyancy members.

Design pressure is given by the multiplication of a characteristic pressure P_k by a partial safety factor for loads γ_f

$$P_{sd} = P_k \cdot \gamma_f \quad (18)$$

DNV-OS-C101 [12] recommends a safety factor for the ultimate limit state (ULS) of $\gamma_f = 1.3$ on environmental loads.

Given that WECs are generally designed to provide maximal response to wave loading (except perhaps if separate survivability modes are defined), it is expected that extreme environmental loads for WECs would be higher than those for an offloading buoy.

As a first approximation, the following relations from DNV-OS-E403 [10] are used but a larger safety factor of 2.0 is assumed to cover the higher expected uncertainties in the loads calculation described above. Note that a separate safety factor is also applied for the material strength defined in section 7.2. For a real assessment, it would be recommended to carry out detailed numerical modelling and physical testing to calculate loads and define suitable safety factors.

Main deck:

$$p_{di} = 10 \left(1 - \frac{d_i}{D} \right)^{0.25} (1 + 0.05L) \quad (kN / m^2)$$

Sides (from main deck to still-water level):

$$p_{si} = p_{di} + 10\gamma(D - z_b) \quad (kN / m^2)$$

Bottom and sides (below still-water level):

$$p_{bsi} = 10\gamma(D - z_b) \quad (kN / m^2)$$

d_i = vertical distance in m from the waterline to the main deck.

L = characteristic maximum horizontal length in m at the still-water draft level.

D = vertical distance in m from the moulded baseline to the main deck, or may alternatively be replaced by the largest relative distance from the moulded baseline to the wave crest if this is proved smaller.

γ = reduction factor due to motion of wave particle (0.9 unless otherwise documented).

z_b = vertical distance in m from the baseline to the load point.

The buoy shown in Figure 3-1 consists of a straight cylindrical shell with a rounded hemispherical cap on the base. The top of the cylinder is closed by a flat circular plate.

The design pressure will vary with depth, so a series of locations are chosen for the load calculation. For the current study the calculation is made for the four locations described in Table 7.1, where the top and bottom halves of the cylinder are considered separately. For future work it would be advisable to divide the geometry into a larger number of sections in order to achieve a more accurate estimate for buoy mass.

Location	Vertical distance from top deck (m)	Vertical distance from still water level (m)
Top deck	0	0.187
Top half of cylinder	0.125	0.062
Bottom half of cylinder	0.25	-0.063
Bottom of hemisphere	0.5	-0.313

Table 7.1 Description of locations for pressure calculation (model scale)

Figure 7-1 shows the calculated design pressures with varying diameter the buoy for the range of device scales k (note the buoy height also scales with k). The figure also shows the calculation results for still-water hydrostatic pressure at the base of the buoy and an approximation for wave slamming pressure at the top part of the cylinder for comparison.

Still water hydrostatic pressure is calculated as:

$$L_{avg} = \rho g z \quad (19)$$

where $\rho = 1025 kg/m^3$ is the water density, $g = 9.81 m/s^2$ and the water depth $z = 0.313 m$ for the model scale.

Wave slamming pressure is approximated following DNV-RP-C205 [11]. The empirical relations were originally defined for wave slamming impact on fixed slender structures, so it is expected that these will be highly approximate for a WEC buoy that is relatively unrestrained in surge. However, the method is deemed sufficient for the current approximate calculation of structural mass considering that an increased safety factor on loads is also assumed. Note that it would be highly recommended in a real design situation to investigate this type of loading based on detailed numerical modelling and physical testing.

Slamming pressure at the start of impact is given by

$$P_s = \frac{1}{2} \rho C_{pa} v^2 \quad (20)$$

where the pressure coefficient at the start of impact is $C_{pa} = 5.15$ and v is the relative impact velocity between water and cylinder.

Assuming the buoy to be initially stationary, the impact velocity is taken to be equal to 1.2 times the wave celerity c [11], where

$$c = \frac{gT}{2\pi} \quad (21)$$

T is taken to be the wave period for the highest breaking wave in n years. The largest breaking wave is taken as 1.4 times the largest significant wave height in n years (from section 8.8.1.2 of [11]). For the current analysis it is assumed that the highest breaking wave can be taken as the largest wave in the 34 and 30 year hindcast data provided for the WETS and EMEC sites respectively [7][8].

The maximum value in the 30 and 34 year hindcast is used as a first estimate for the 30 year return value. For subsequent work it would be suggested to carry out more detailed analysis of return values using extreme wave analysis (i.e. by fitting a distribution to the data and extrapolating).

The largest significant wave height for the WETS site is taken as $H_s=5.625m$ and for the EMEC site as $H_s=11.4m$.

The period of the largest breaking wave is calculated by assuming a limiting wave steepness of

$$\frac{H}{\lambda} = 1/7$$

Where the wavelength is

$$\lambda = \frac{gT^2}{2\pi}$$

After some rearranging, the wave period is given by

$$T = \sqrt{\frac{2\pi \cdot 7 \cdot 1.4 H_s}{g}} \quad (22)$$

And the impact velocity is

$$v = 1.2 \sqrt{\frac{7 \cdot g \cdot 1.4 \cdot H_s}{2\pi}} \quad (23)$$

The wave period for the breaking wave is calculated as 5.9s for WETS and 8.5s for EMEC. The associated impact speed is calculated as 11.1m/s and 15.8m/s for the two sites respectively.

Figure 7-1 and Figure 7-2 show the design pressures with scale for the four sections of the buoy listed in Table 7.1, for the WETS and EMEC site. It is noted that the equations for design pressure from DNV-OS-E403 include hydrostatic pressure even for the section above the still water line because it is assumed that the buoy can be fully submerged by a wave. The hydrostatic component of pressure becomes increasing important for larger scale structures as the draft increases.

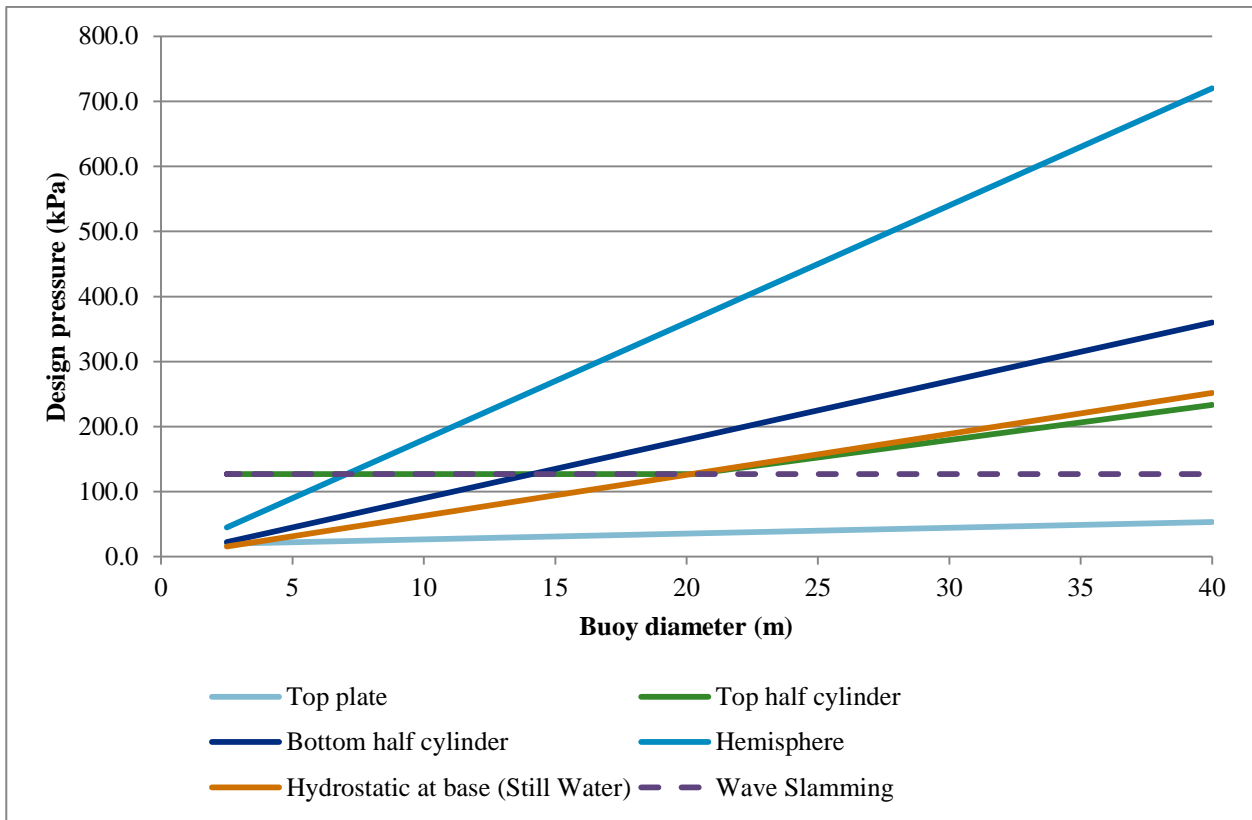


Figure 7-1 Factored design pressures on shell sections for varying buoy diameter for WETS

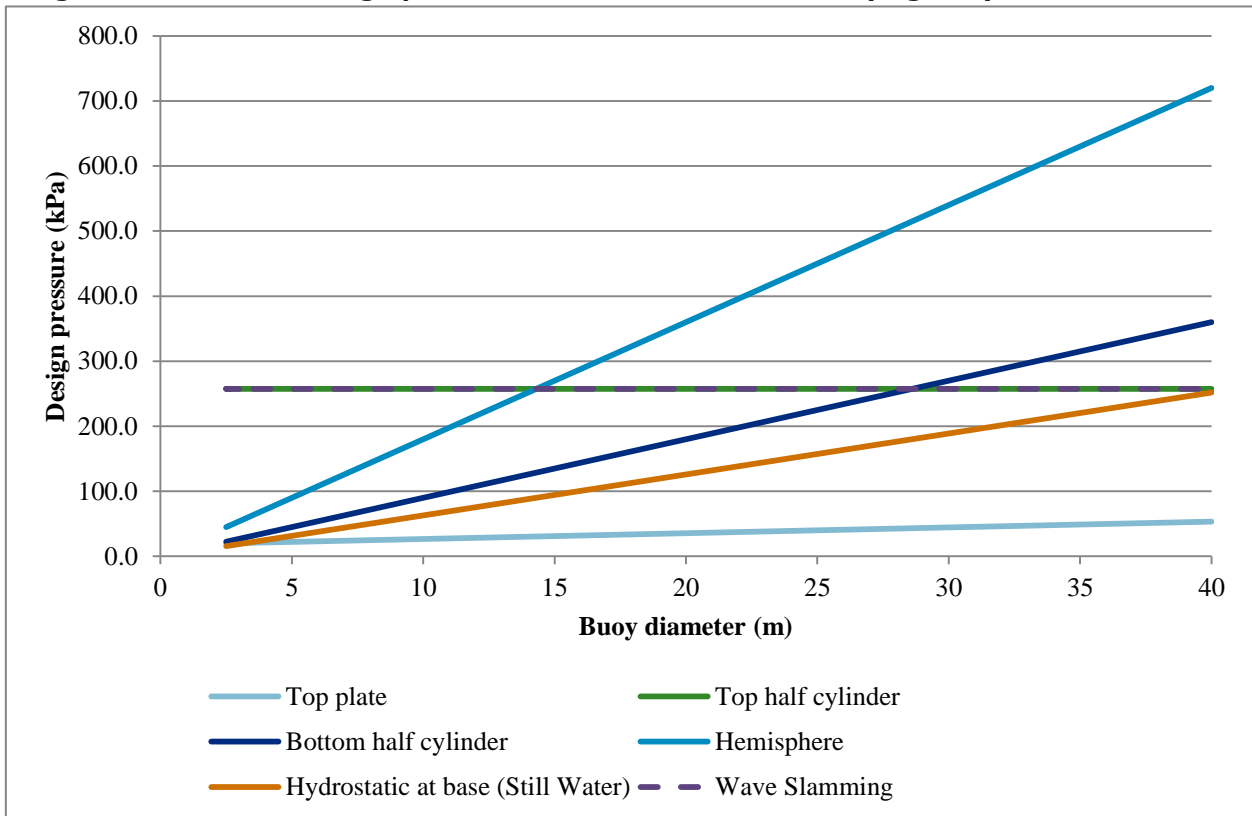


Figure 7-2 Factored design pressures on shell sections for varying buoy diameter for EMEC

7.2 Plate thickness requirement

It is assumed that the design pressures described in section 7.1 above are uniformly distributed around the cylinder/sphere. In reality wave pressures would induce non-axisymmetric loading, leading to local bending stresses in the shells, however for the purposes of an approximate sizing calculation this is neglected.

From experience, the thickness requirement of thin cylindrical and spherical shells under external pressure is expected to be driven by buckling. The thickness calculation is therefore estimated based on design equations from DNV-RP-C202, 'Buckling strength of shells' [14] and DNV classification note 30.3, 'Buckling criteria of LNG spherical cargo tank containment systems' [15].

A realistic design would be expected to have at least some internal stiffening, for example vertical stiffeners at 90degree or 45degree intervals and possibly ring stiffeners at the top and bottom of the cylinder. The inclusion of stiffeners would allow for a thinner outer shell in regard to buckling strength, but the stiffeners would themselves add some weight to the structure. A stiffened shell should be lighter in weight overall, but for the purpose of estimating approximate mass of the structure; it is expected to be sufficient to base the buckling calculation on the simpler equations that assume un-stiffened shells.

Circumferential membrane stress in an unstiffened cylinder is given by [21]

$$\sigma_{h,sd} = \frac{P_{sd} \cdot r}{t} \quad (24)$$

where r is the mean radius, t is the thickness and P_{sd} is the design pressure (see section 7.1 above)

The membrane stress in an unstiffened hemisphere shell is given by [21]

$$\sigma_{h,sd} = \frac{P_{sd} \cdot r}{2t} \quad (25)$$

The intention is to find a shell plate thickness t such that the following condition is satisfied

$$\sigma_{h,sd} \leq f_{ksd} \quad (26)$$

or for cylindrical shell

$$t \geq \frac{P_{sd} \cdot r}{f_{ksd}} \quad (27)$$

where $\sigma_{h,sd}$ is set equal to design buckling strength f_{ksd} , which is defined in section 3.1 of [14] as

$$f_{ksd} = f_{ks} / \gamma_m \quad (28)$$

The material factor γ_m is conservatively taken to be 1.45 [14].

For the cylindrical shell, the characteristic buckling strength f_{ks} is calculated using

$$f_{ks} = \frac{f_y}{\sqrt{1 + \bar{\lambda}_s^4}} \quad (29)$$

The characteristic material yield strength f_y is assumed to be 235MPa and for purely axisymmetric circumferential compression the $\bar{\lambda}_s$ is a slenderness parameter given by

$$\bar{\lambda}_s = \sqrt{\frac{f_y}{f_{Eh}}} \quad (30)$$

The characteristic buckling strength for unstiffened circular cylinders under purely axisymmetric circumferential compression is

$$f_{Eh} = \frac{C\pi^2 E}{12(1-\nu^2)} \left(\frac{t}{l}\right)^2 \quad (31)$$

Where l is the length of the unsupported cylinder ($l=0.25m$ at model scale), t is the thickness, the modulus of elasticity for steel E is $E=210GPa$, the Poisson's Ratio $\nu = 0.3$, and the reduced buckling coefficient C is given by

$$C = \psi \sqrt{1 + \frac{\rho\zeta}{\psi}} \quad (32)$$

Where the buckling coefficients in the above equation are defined in Table 3-2 of [14], as $\psi=2$, $\rho = 0.6$, and

$$\zeta = 1.04 \sqrt{\frac{l^2}{r \cdot t} \sqrt{1-\nu^2}} \quad (33)$$

Where the remaining parameters are already defined above.

Given that equation (31) and (33) include the cylinder thickness, it is not possible to satisfy the inequality in equation (27) directly. Therefore, the required shell thickness for buckling strength is calculated by iteration of the above formula. This process is repeated for the range of scales of the WEC device.

A similar process for calculating the characteristic buckling strength for the hemispherical shell is carried out following Section 4 of [15].

The thickness of the top circular plate is calculated based on standard formula for bending stress at the centre of a uniformly loaded flat circular plate. The edges are conservatively assumed to be simply supported.

$$\sigma_p = \frac{1.238Pr^2}{t^2} \quad (34)$$

Rearranging this equation and assuming a material factor of $\gamma_m = 1.1$ for on the plate yield strength, the required plate thickness is calculated as

$$t = \sqrt{\frac{1.238 \cdot P \cdot r^2}{f_y/\gamma_m}} \quad (35)$$

7.3 Structural mass

Figure 7-3 shows the calculated shell thickness requirement for buckling strength for the range of buoy sizes, for the WETS and EMEC sites. It can be seen that the thickness of the top half of the cylinder differs for the two sites due to the different conditions for the wave slamming design pressures.

Note that a limit on the minimum thickness has been defined from DNVGL-OS-C201 [13]

$$t_{min} = 15.3 \frac{t_m}{\sqrt{f_y}} = 6.98mm \quad (36)$$

where $t_m = 7mm$, $f_y = 235MPa$



It can be seen from Figure 7-3 and Figure 7-4 that the calculated thickness requirement of the shell reaches extremely high values of 190mm for the largest scale devices. This plate thickness is unrealistically large and not sensible for fabrication purposes. Instead internal stiffeners would be used to allow for reduced shell thickness. Stiffeners themselves would contribute some mass, but would lead to a lighter design overall. The current calculations are considered sufficient for an initial and conservative estimation of required structural mass.

Figure 7-5 and Figure 7-7 show a breakdown of the calculated structural mass for the cylindrical and hemispherical shells and top plate, for the WETS and EMEC site. The mass is computed by multiplication of the surface area by the calculated shell thickness, for the range of device scales. The total structural mass is also shown in each figure. Figure 7-7 shows a comparison of the calculated total mass for the two sites for the full range of diameter scales and for clarity, Figure 7-8 show the same results but over the range of 2.5 to 15m diameters. It can be seen that the total mass is larger for the EMEC site than at WETS due to the higher wave slamming pressure, however this difference is not very large because the top section of the cylinder only makes up about a third of the total mass of the device.

To check that these mass values are feasible, a comparison is made with the mass for two reference WEC devices. Babaret et. al. [17] lists the mass for a 3m diameter bottom-referenced heaving buoy as 1 tonne. The calculated total structural mass for a 3m diameter buoy from Figure 7-8 is approximately double this value at around 2 tonnes.

The mass of a much larger device, the 20m diameter surface float of the DOE two-body point absorber 'RM3' reference model is listed as 207tonnes in the Sandia National Laboratories report [18]. From Figure 7-8, the corresponding mass for the current generic single-body point absorber buoy is approximately 520 tonnes for the WETS site and 570 tonnes for the EMEC site. The present model is a factor of 2.5 larger. This may be due to the increased safety factors used in the current calculations and the fact that the design is not optimised with the use of stiffeners. Furthermore, the present generic WEC has a much deeper draft than the surface float used in the DOE model, which means that a larger proportion of the buoy is subject to higher hydrostatic loads. The current method for calculating structural mass is deemed to be suitably accurate for use in the present high-level study of cost per MW, discussed in section 8.

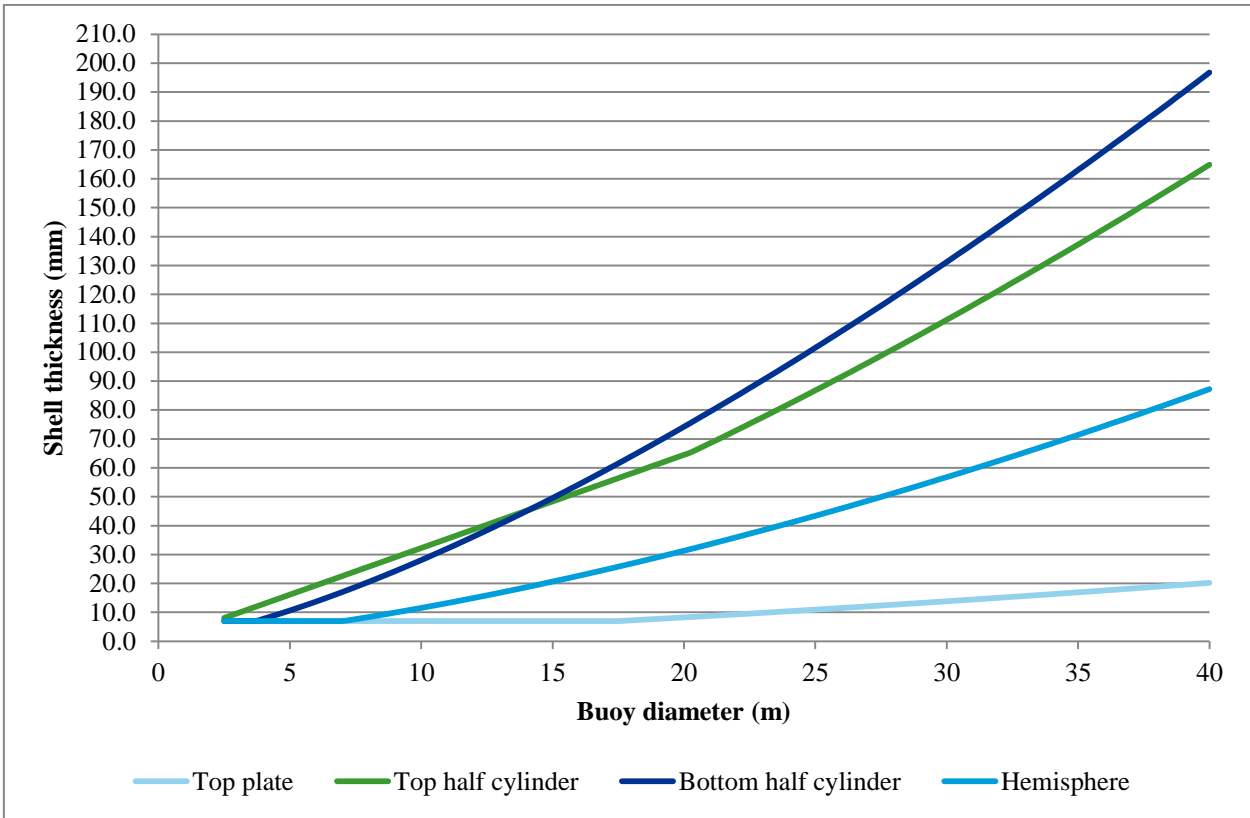


Figure 7-3 Calculated thickness of shell sections for varying buoy diameter (WETS site)

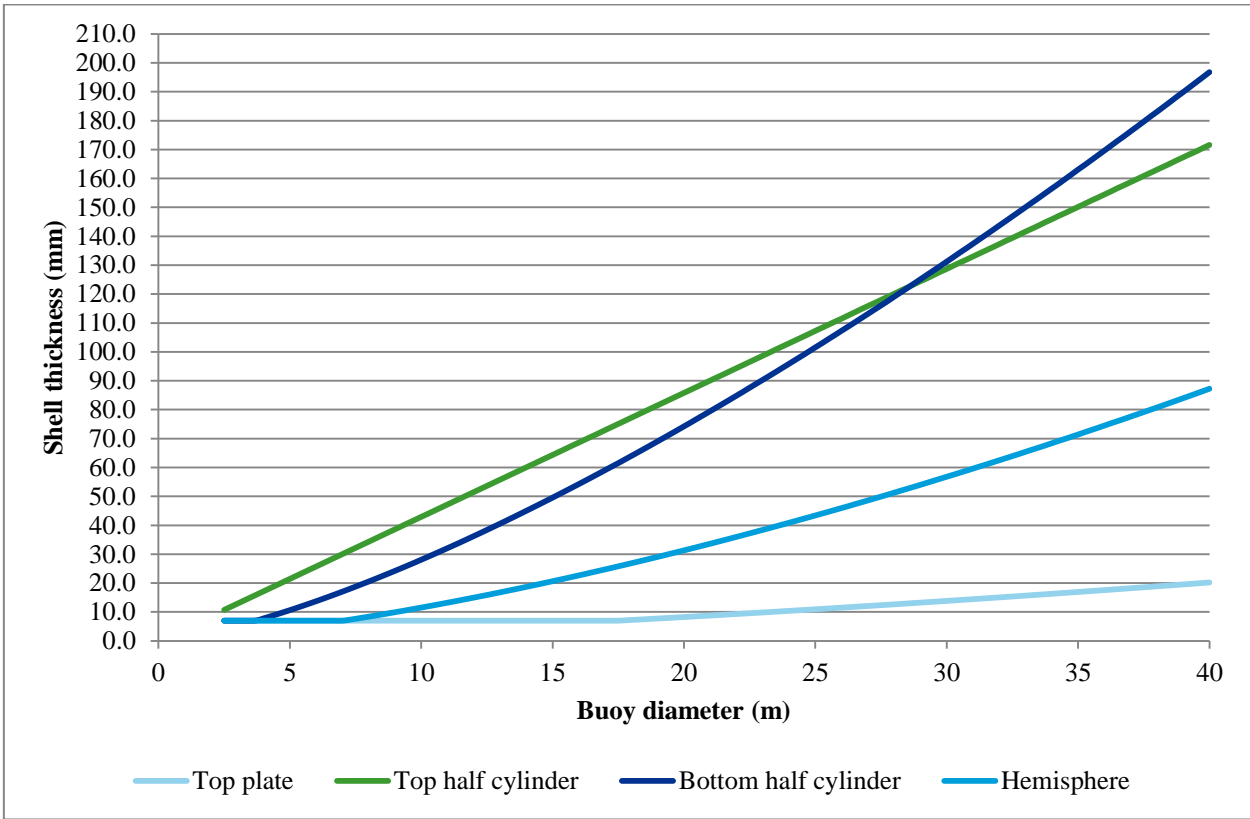


Figure 7-4 Calculated thickness of shell sections for varying buoy diameter (EMEC site)

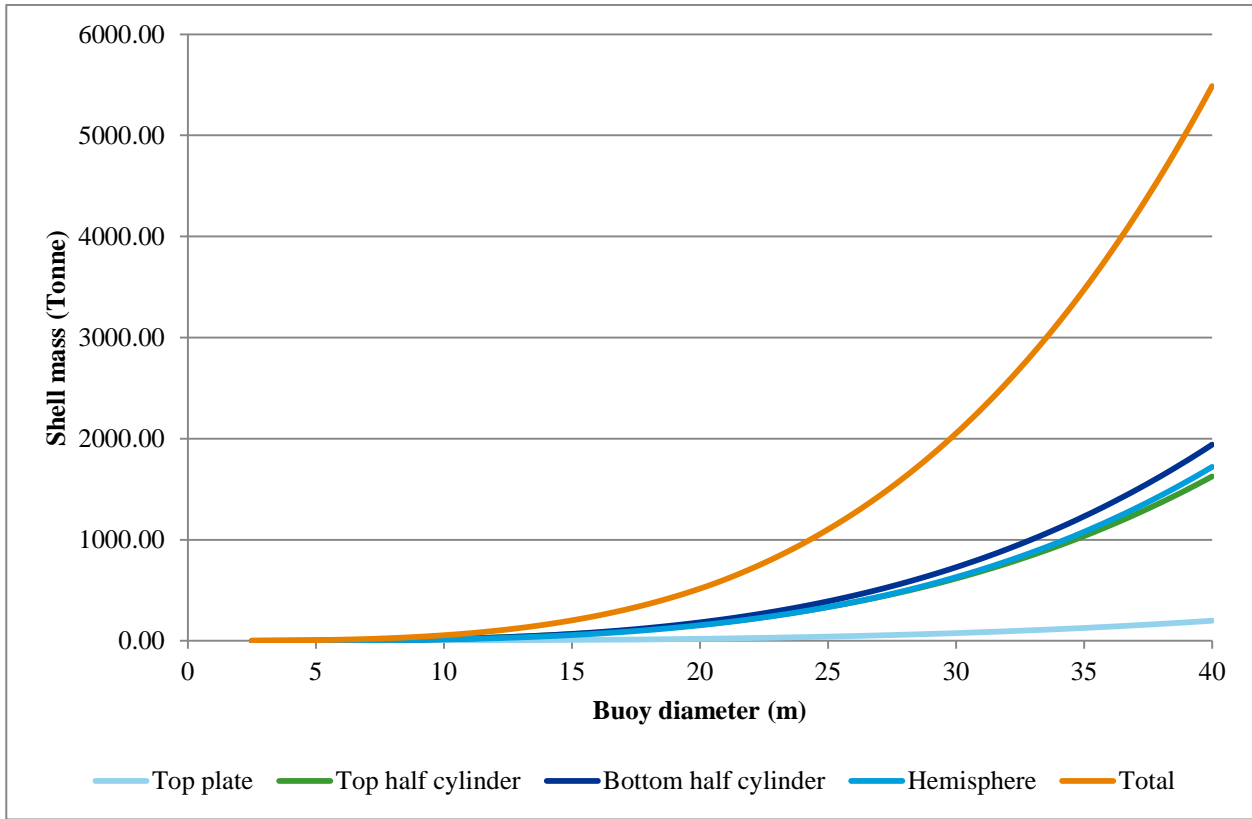


Figure 7-5 Calculated mass of shell sections for varying buoy diameter (WETS site)

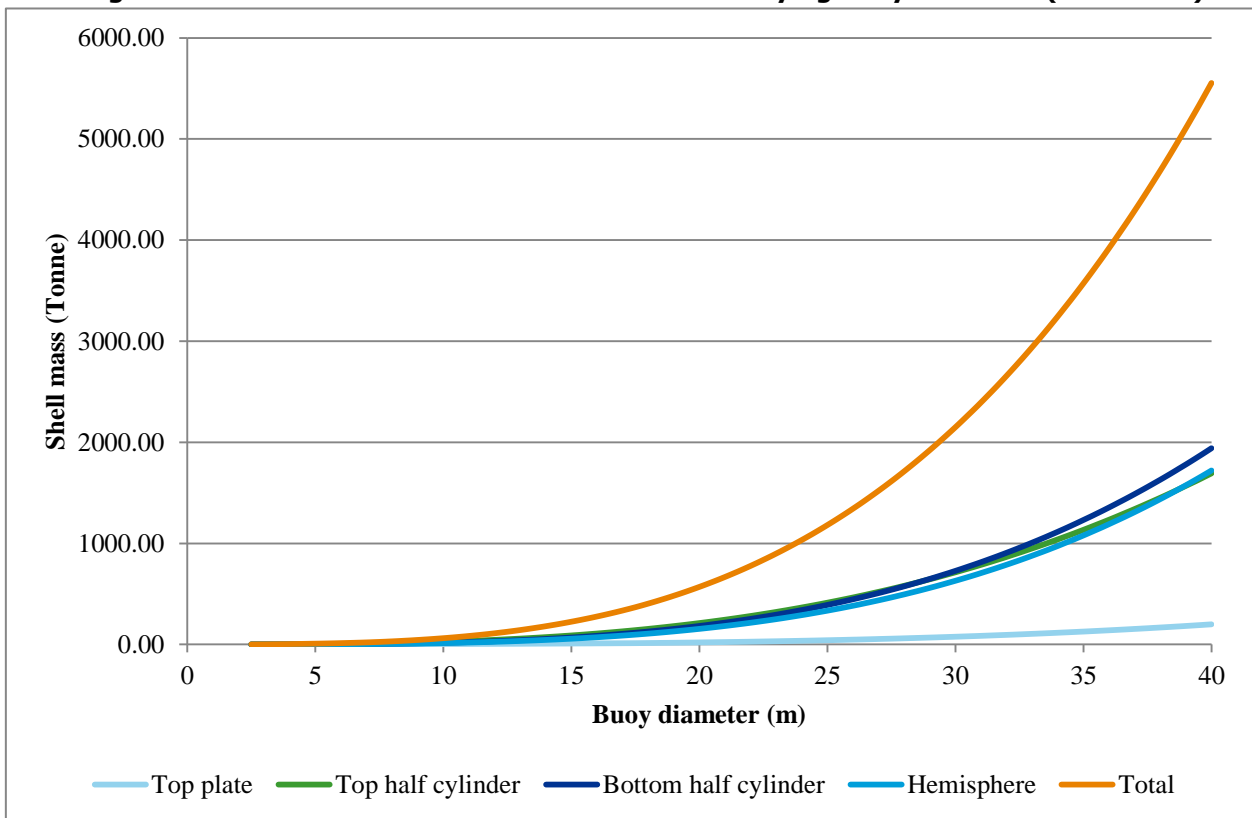


Figure 7-6 Calculated mass of shell sections for varying buoy diameter (EMEC site)

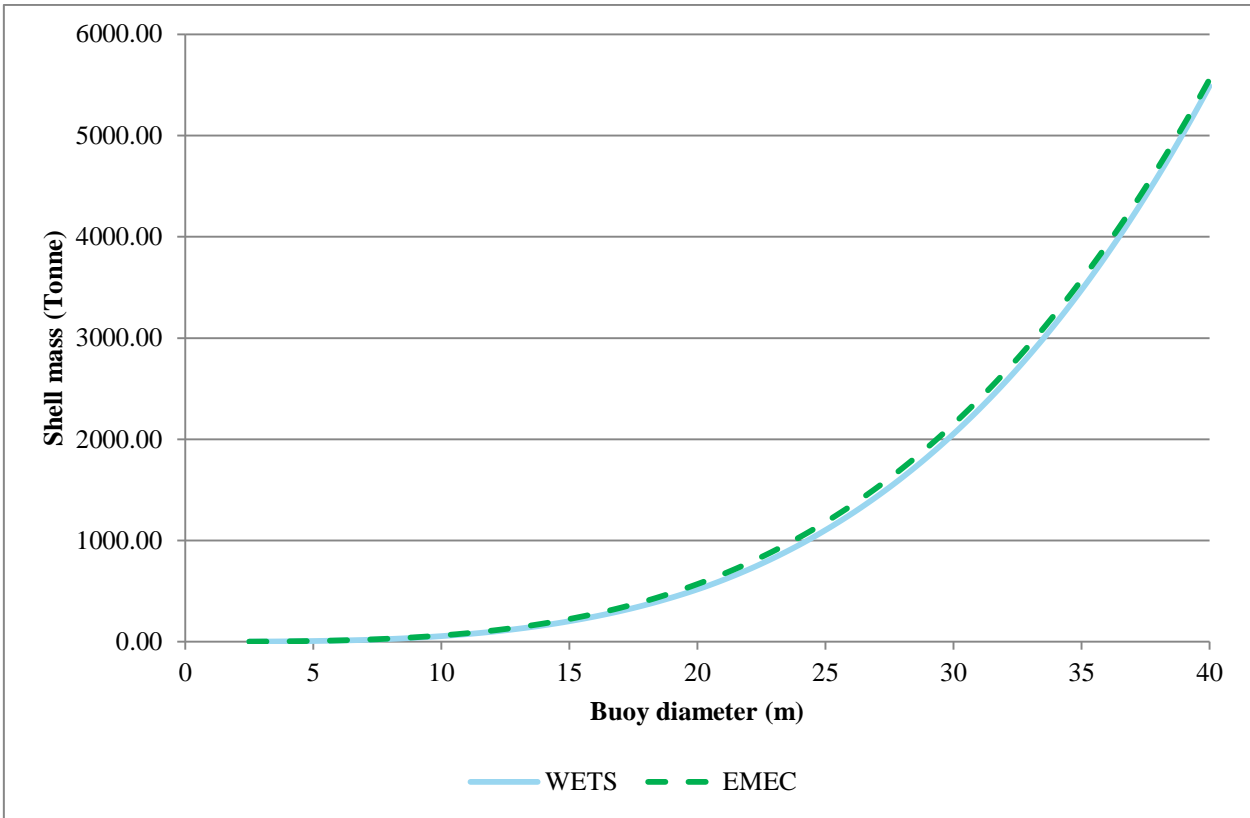


Figure 7-7 Calculated total mass of buoy for WETS and EMEC site (0-40m diameter range)

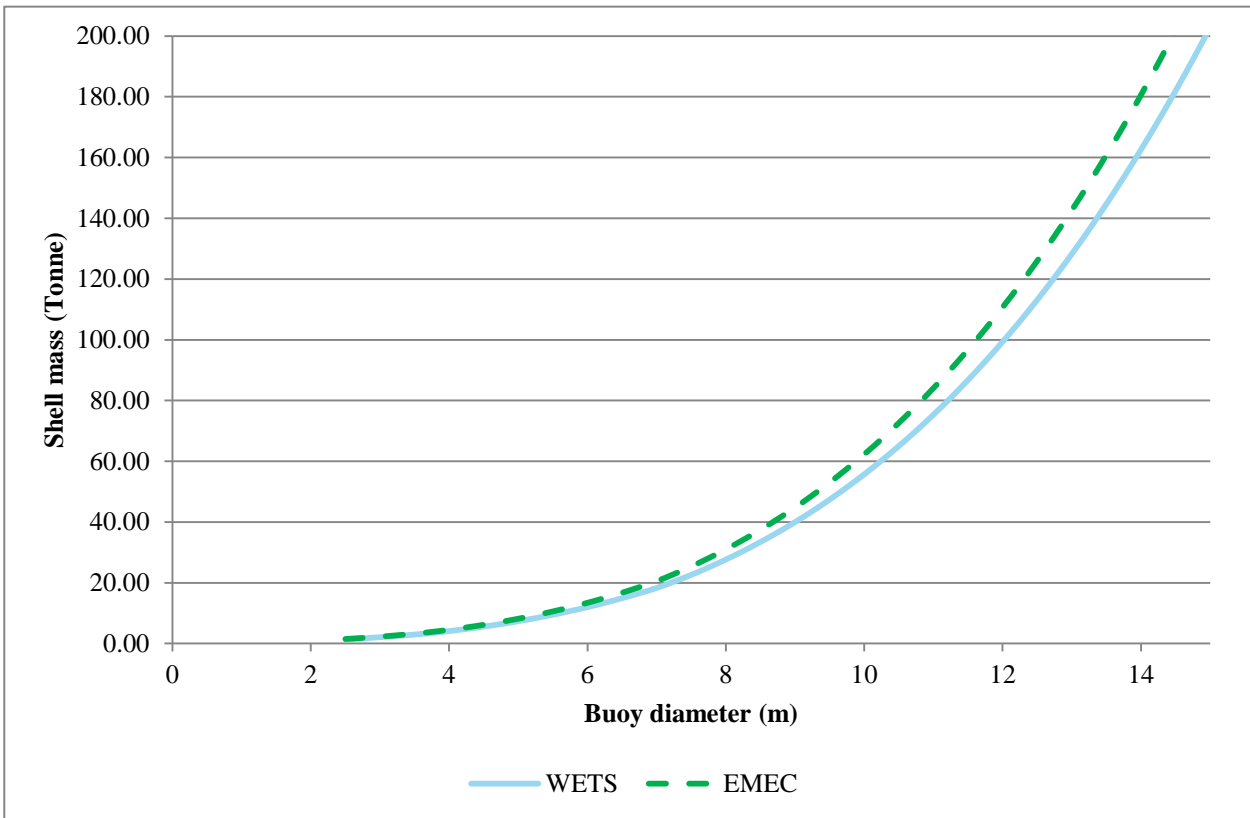


Figure 7-8 Calculated total mass of buoy for WETS and EMEC site (0-15m diameter range)

Figure 7-9 below shows how mass would vary with buoy diameter if the thickness were also to scale linearly with k . (i.e. assuming Mass scales with k^3). The total mass calculated from the design code for the 20m device is used as the reference mass for scaling.

$$M_k = M_{k=20} \left(\frac{k}{k_{20}} \right)^3$$

It can be seen that the mass of the buoy scales at a slightly higher rate than the k^3 . Rather, it appears that the calculated shell mass scales approximately with an exponent of 3.4. This case provides an example where it is helpful to carry out at least simple structural calculations to identify and understand what loading conditions may control the requirement for structural material. A similar process might also be carried out using simple sizing calculations for components such as the mooring line, PTO etc.

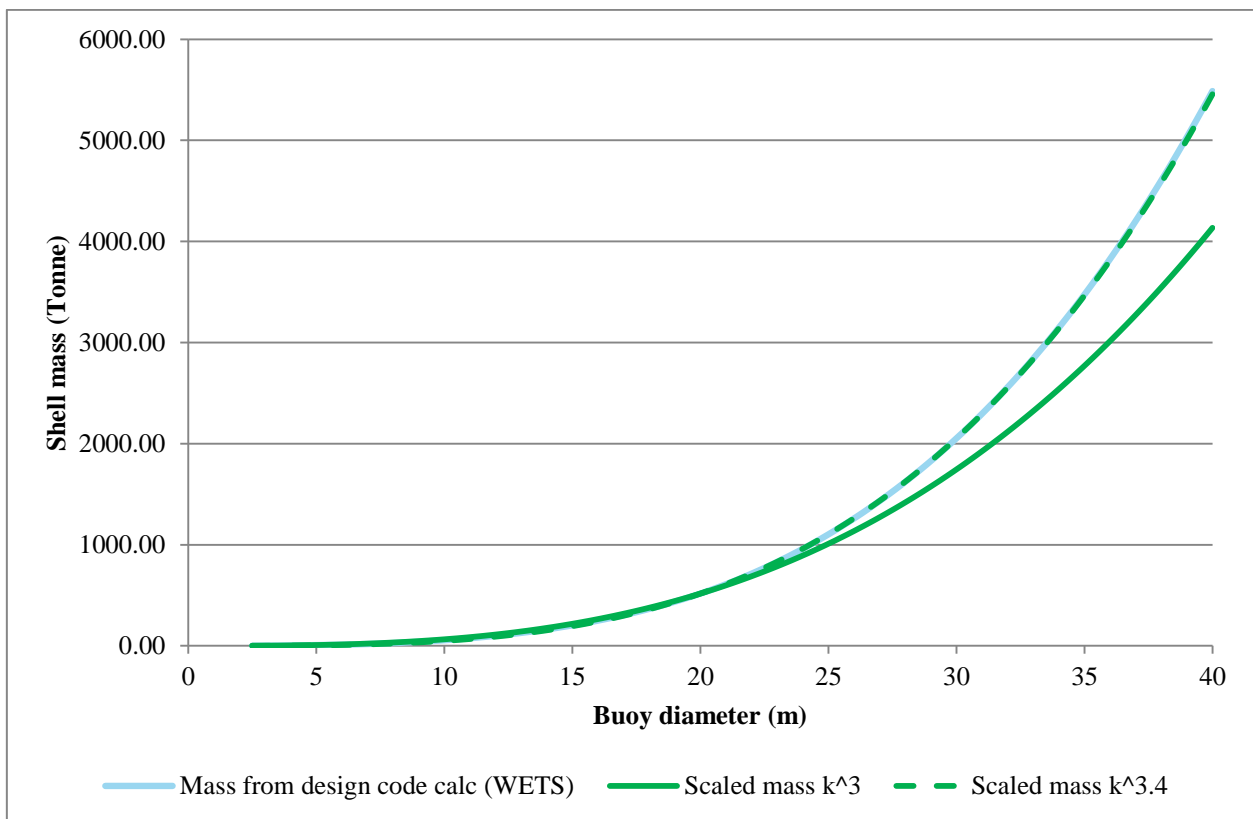


Figure 7-9 Comparison of calculated buoy mass to scaled mass assuming $M_k = M \times k^3$

8 COST PER MW OF RATED POWER OUTPUT

HNEI has expressed interest in understanding whether different optimum scales of device can be chosen for different site locations in regard to both relative power performance and cost for survivability [5].

Assessment of costs is commonly based on Levelised Cost of Energy (LCOE), which includes detailed analysis of various capital costs (e.g. WEC fabrication, foundation, installation etc.), operational costs and balance of plant costs.

This study intends to illustrate an approximate approach for comparing and selecting suitable device scales based on the metric *cost per MW of rated power output*. This focuses on dividing the costs into those that scale with device size and those that are relatively independent of scale (termed here as 'fixed' costs). The fabrication costs of various main components of the WEC, such as the main floating structures, Power Take-Off (PTO) unit, mooring lines etc. may scale with the mass of the material requirement. However, the components which are needed for every device irrespective of the scale of the device (within certain ranges) are categorized as 'fixed costs'.

The estimation of required mass of structural steel is demonstrated in section 7.3 for the main buoyant unit of the generic point absorber device. Similar calculations can be made for other components such as the mooring/tether, foundation, PTO etc. and each of these would be expected to exhibit slightly different scaling rules. For the purposes of this study, the scale-dependent costs will be based only on the fabrication costs of the buoy. Manufacturing costs for a range of fabricated steel substructures for floating wind are listed in [19], which provides an average value of \$2300 per tonne. A conservative estimate of fabrication cost per tonne of steel for the main float structure of the generic WEC is therefore taken to be \$3000 per tonne. For reference, Tables 5-6 and 5-10 and Figure 5-26 of [18] lead to a figure in the range \$2,500/tonne - \$4,200/tonne for the costs of the float column and plate of the WEC.

Figure 8-1 provides a general prediction of the contribution of different cost types to overall LCOE for a wave array. It can be seen that approximately a third of the total LCOE relates to the structure and about a quarter relate to the PTO, foundation and mooring.

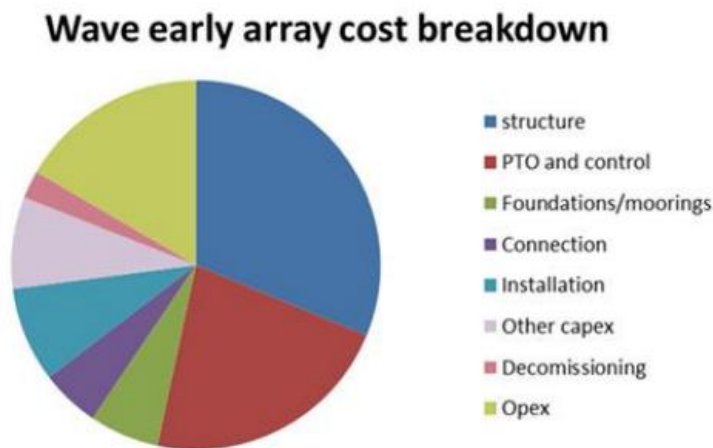


Figure 8-1: Wave early array cost breakdown [20]

As a rough approximation, it will be assumed that the buoy structure accounts for a third of the total scale-dependent costs (not the total LCOE shown in Figure 8-1). The total cost is therefore given by

$$Total\ Cost = Structural\ Mass \cdot \left(\frac{\$3000}{Tonne} \right) \cdot 3 + Scale\ Independent\ Costs \quad (37)$$

The cost per MW of rated power is given by

$$\text{Cost per MW (rated power)} = \frac{\text{Total Cost}}{\text{Annual Mean Power/Capacity Factor}} \quad (38)$$

A capacity factor of 0.3 is assumed here. This accounts for the fact that the output of a WEC device is highly variable and will not be available for energy production throughout the whole year and as such the device will produce less than the rated power on average. Therefore the rated power is set higher than the estimated annual mean power.

The scale independent or 'fixed' costs are a significant unknown. The current approach will aim to illustrate how the cost per MW of rated power varies with different levels of fixed costs. This is helpful for understanding the relative influence of different fixed and scale-dependent costs on optimum scale for different sites. Furthermore, it will provide a basis for future interpretations if data is available on expected fixed costs for an actual device and site. This approach may be particularly relevant to wave energy test centers, where much of the infrastructure has already been installed and as such information regarding the various fixed costs may already be known.

Figure 8-2 shows the calculated Cost per MW rated power for a series of device scales at the WETS and EMEC site. Curves are shown for a range of non-scalable costs per device from zero to \$500,000. The solid lines refer to the WETS site and the dashed lines relate to the EMEC site.

It is interesting to first consider the special case of zero fixed costs. In this case, the Cost per MW rated power is purely defined by the ratio of the calculated fabrication mass of the buoy and the calculated power output for each scale. The buoy mass is shown in section 7.3 to vary approximately with $k^{3.4}$. Based purely on Froude scaling laws, power scales with $k^{3.5}$, but as shown in Figure 6-1 and discussed in section 6, the power output is also influenced by the varying resonant period of the device with scale, relative to the average annual spectrum at each site.

From Figure 8-2, it can be seen that for zero fixed cost, the Cost per MW for the WETS site shows a minimum at around 5.5m diameter. For the EMEC site, the Cost per MW is shown to be minimum at the smallest scale of 2.5m diameter, however it can be seen that the shape of the curve is not smooth at this location, so it is possible that this local minimum may be affected by small numerical inaccuracies. As the shape of the Cost per MW (zero fixed cost) curve for the EMEC site is relatively flat over a quite a wide range of diameters (i.e. 2.5m to 7.5m), it is possible that the diameter for the actual minimum could be also be closer to 5m and therefore similar to the WETS site. This current study is useful to generally illustrate which range of scales may provide the lowest Cost per MW and could be used as the basis for further work investigating a narrower band of scales with additional accuracy.

In reality there will always be some element of fixed cost, so it is helpful to look further at how Cost per MW changes with varying fixed cost, in Figure 8-2.

It can be seen that for each level of non-scalable cost, the combined Cost per MW is consistently higher at the WETS site compared to the EMEC site. This may be expected given that the annual mean power is already shown in Figure 6-1 to be consistently higher for the EMEC site than the WETS site.

It is also interesting to note that the cost per MW increases dramatically with reducing scale for very small sizes below 5-10m diameter, depending on the level of fixed cost. This is explained by the fact that the scale-dependent cost becomes small relative to the fixed costs for small devices, so the fixed costs dominate the overall cost of small scale devices. If the overall cost is fixed for small scale devices, but the power output continues to reduce with reducing scale, then the cost per MW of power must increase.

At scales larger than about 5 to 15m, the cost per MW increases for all levels of fixed cost and these tend to converge to a single gradient for very large diameters. This is because the scale-dependent costs become dominant compared to the specified fixed costs. Interestingly, the difference between results for the WETS and EMEC sites becomes increasingly different for larger scales above about 15m diameters, which is a consequence of the larger devices being able to extract energy from more powerful, long waves that are available at the EMEC site.

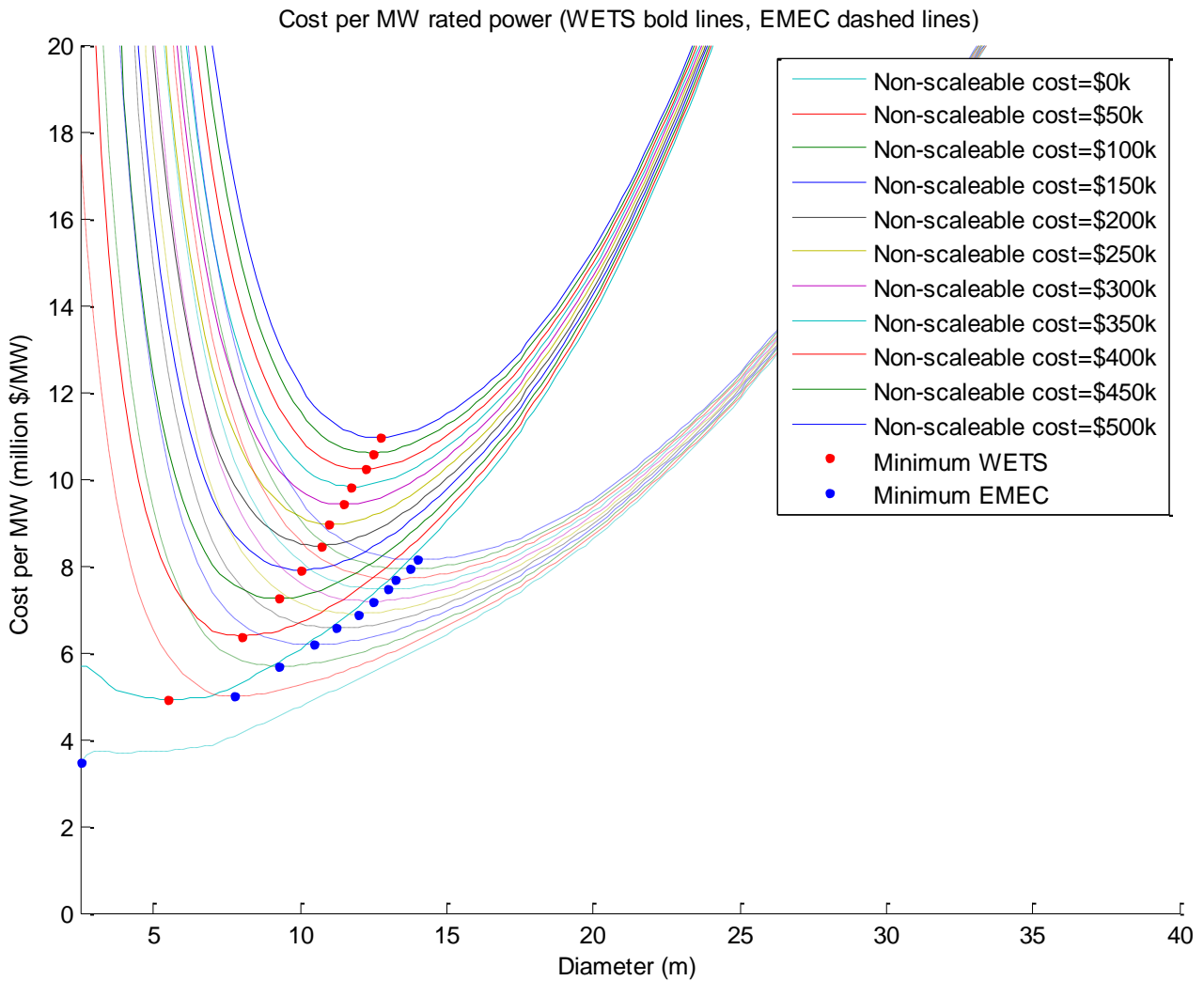


Figure 8-2: Cost per MW rated power for varying buoy diameter and level of non-scalable costs (bold lines: WETS site, dashed lines: EMEC site)

For each level of fixed cost in Figure 8-2 there is a minimum value of *Cost per MW*. Figure 8-3 identifies the buoy diameter at which each of these minima occur for each of the levels of non-scalable cost, for both the WETS and EMEC site. Figure 8-4 shows the associated minimum cost per MW for various levels of non-scalable cost. Although the term 'optimum' is used here, it is emphasized that this is only in respect to the *Cost per MW* criteria in this study (i.e. other criteria may also be important in terms of design such as limits on size and capacity of manufacturing facilities, transport links etc.).

As mentioned above, for the special case of zero fixed costs, it is expected that the identified optimum diameter for the EMEC site may be affected by numerical inaccuracies. As zero fixed cost is an unlikely scenario, it is suggested that this value should be disregarded. From \$50k to \$150k fixed cost, the optimum diameter is very slightly larger for the WETS site than at EMEC, but the difference is less than 0.25m, so again may be insignificant in regard to numerical inaccuracies. What is interesting to note for fixed costs above \$150k is that the optimum diameter stays within the range of 10 to 14m for both the WETS and EMEC sites, up to the largest fixed cost considered. The optimum size is larger at the EMEC site for a fixed cost of \$500k, but only by 1m in diameter.

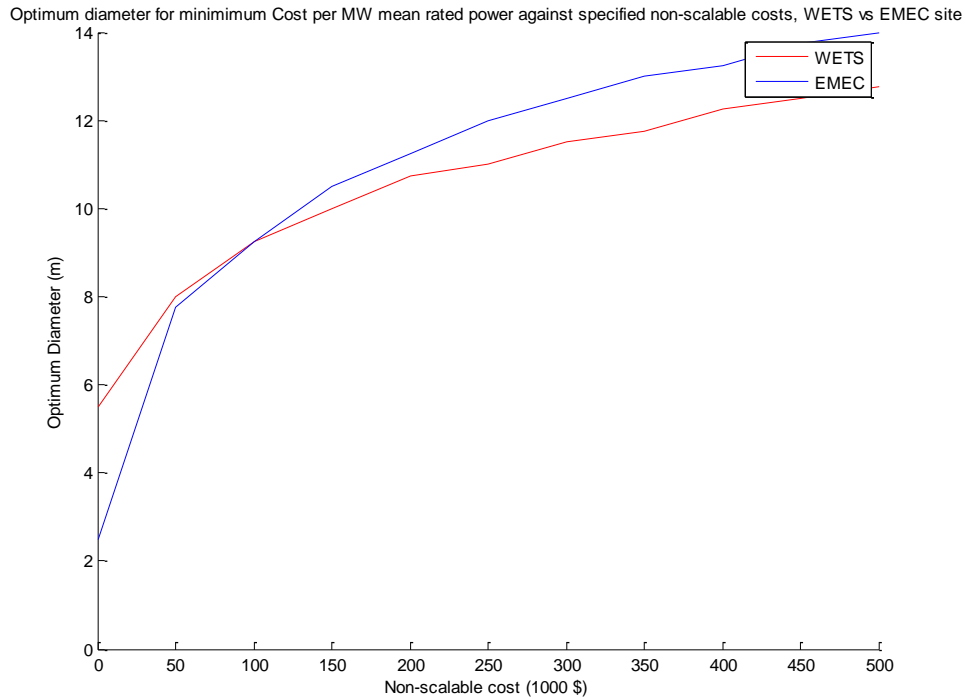


Figure 8-3: Buoy diameter for identified minimum cost per MW rated power, against level of non-scalable costs (red line: WETS site, blue line: EMEC site)

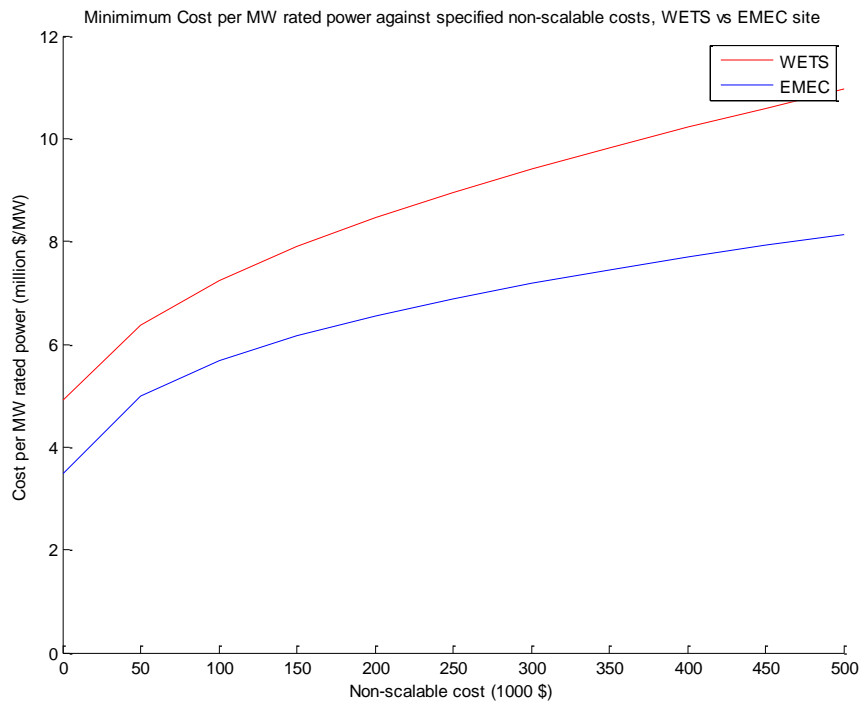


Figure 8-4: Minimum cost per MW rated power against level of non-scalable costs (red line: WETS site, blue line: EMEC site)

9 CONCLUSIONS

This technical note has presented a methodology and along with a tentative application for choosing an appropriate size of device for a given site. The following conclusions may be drawn from this exercise:

- A time-domain numerical model has been created of a *generic rounded cylinder single-body point absorber* in DNV GL's WaveDyn WEC design tool and run for a broad array of unidirectional sea states. This model can be used by HNEI to verify their own numerical models. More detailed results will be presented in subsequent deliverables.
- The model represents a relatively simple type of WEC, which can be used to gain understanding on general WEC behaviors.
- Absorbed power values have been extracted from the WaveDyn model and post-processed to provide a relationship between mean annual power with scale of device for two wave energy test sites, WETS and EMEC. These illustrate that the power is heavily influenced by the varying resonant period of different scales of device, relative to the defined annual average wave spectrum at the site.
- A simple sizing exercise has demonstrated a methodology to approximate the mass requirements of steel for the main WEC float, based on methods from existing offshore design standards for the ultimate limit state. There is considerable uncertainty in applying these methods to the design of wave energy converters, so a number of conservative assumptions have been made. It is found for the current WEC that mass approximately scales with $k^{3.4}$, where k is the scale factor, rather than k^3 which would be expected if thickness were to scale in proportion to the other dimensions. The increased exponent appears to derive from the fact that



a significant portion of the assumed loading on the buoy comes from hydrostatic pressure, which increases with scale because of the increasing draft of the structure.

- A simple study has been carried out into the relationship of cost per MW rater power with scale of the device. Results are expected to be approximate, but it is generally found that the currently considered device may have an optimum diameter in the range of 5 to 15m, depending on the level of fixed costs at the installation site. The identified optimum diameter is very similar for the WETS and EMEC site. The associated cost per MW is shown to be higher at the WETS site compared to the EMEC site.

Although approximate, the current study highlights that it is important to consider both power production and cost of structure when choosing suitable scales of device. It is tempting to chase ever higher power output by designing larger devices to survive more energetic wave conditions, but in regard to cost per MW, smaller to medium size devices may be more favorable, depending on the device. It should be noted that the current sizing calculations do not attempt to consider fatigue strength, which may also be critical for design of WECs.

During this study it has been noted that calculations have been carried out assuming deep water criteria is satisfied (i.e. in order to neglect scaling of water depth). For future work it is recommended to run the WaveDyn model at a defined scale with the correct site water depth defined.

10 REFERENCES

- [1] Agreement for services and RCUH P.O #Z10027978, 15 April, 2013
- [2] Amendment No. 1 to the services agreement between the Research Corporation of the University of Hawaii and Garrad Hassan America, Inc, 14th August 2014
- [3] Email from Luis Vega to Jarett Goldsmith, 23th October 2015
- [4] Email from Luis Vega to Jarett Goldsmith, 24^h October 2015
- [5] Email from Luis Vega to Jarett Goldsmith, 31th July 2015
- [6] Snatch loading of a single taut moored floating wave energy converter due to focussed wave groups, Martyn Hann, Deborah Greaves, Alison Raby, *Ocean Engineering* 96 (2015) 258-271
- [7] Wave energy resource characterisation at the US Navy Wave Energy Test Site (WETS) and other locations in Hawaii, Ning Li and Kwok Fai Cheung, Department of ocean and resources engineering, University of Hawaii, Nov 2014
- [8] Validation of a thirty year wave hindcast using the Climate Forecast System Reanalysis winds, Arun Chawla, Deanna M. Spindler, Hendrik L. Tolman, *Ocean Modelling*, Volume 70, October 2013, pages 189–206.
- [9] IEC/TS 62600-100, Edition 1.0 (2012-08), Marine energy – Wave, tidal and other water current converters – Part 100: Electricity producing wave energy converters – Power performance assessment
- [10] DNVGL-OS-E403, Offshore Loading Buoys, July 2015
- [11] DNVGL-RP-C205, Environmental conditions and environmental loads, April 2014
- [12] DNVGL-OS-C101, Design of offshore steel structures, general LRFD method
- [13] DNVGL-OS-C201, Structural design of offshore units – WSD method, July 2015
- [14] DNV-RP-C202, Buckling strength of shells, January 2013
- [15] DNV GL Classification Note No. 30.3, Buckling criteria of LNG spherical cargo tank containment systems – skirt and sphere, December 1997
- [16] GL Garrad Hassan Report 702053-USSD-R-01-B, Test Protocols Final Report, Hawaii National Marine Renewable Energy Centre WEC Ocean Testing, 14th May 2013
- [17] Numerical benchmarking study of a selection of wave energy converters, A. Babarit, J. Hals, M.J. Muliawan, A. Kurniawan, T. Moan, J. Krokstad, *Renewable Energy*, Volume 41, 2012, pages 44-63
- [18] Sandia report, Methodology of the design and economic analysis of marine energy conversion (MEC) technologies, Vincent S. Neary, Mirko Previsic, Richard A. Jepsen, Michael J. Lawson, Yi-Hsiang Yu, Andrea E. Copping, Arnold A. Fontaine, Kathleen C. Hallett, Dianne K. Murray, Sandia National Laboratories, 2014
- [19] Levelised cost of energy for offshore floating wind turbines in a life cycle perspective, Anders Myhr, Catho Bjerkseter, Anders Ågotnes, Tor A. Nygaard, *Renewable Energy*, Volume 66, June 2014, pages 714-728.
- [20] Ocean Energy: Cost of energy and cost reduction opportunities, SI Ocean, May 2013

- 
- [21] Roark's formulas for stress and strain, Warren. C Young, Richard G, Budynas, 7th Edition, McGraw-Hill, 2002
- [22] Child, BFM. On the configuration of arrays of floating wave energy converters. PhD Thesis. The University of Edinburgh, 2011.